NASA TECHNICAL NOTE

NASA TN D-8491 c.1

IN SITU MEASUREMENTS OF ARCTIC ATMOSPHERIC TRACE CONSTITUENTS FROM AN AIRCRAFT

Gregory M. Reck, Daniel Briehl, and Ted W. Nyland

Lewis Research Center
Cleveland, Ohio 44135

NATIONAL AERONAUTICS AND SPACE ADMINISTRATION • WASHINGTON D. C. • JUNE 1977

1. Report No.	2. Government Accession No.	3. Recipient's Catalog No.
NASA TN D-8491		

4. Title and Subtitle
IN SITU MEASUREMENTS OF ARCTIC ATMOSPHERIC TRACE CONSTITUENTS FROM AN AIRCRAFT

5. Report Date
June 1977

6. Performing Organization Code

7. Author(s)
Gregory M. Reck, Daniel Briehl, and Ted W. Nyland

8. Performing Organization Report No.
E-9040

10. Work Unit No.
197-10

9. Performing Organization Name and Address
Lewis Research Center
National Aeronautics and Space Administration
Cleveland, Ohio 44135

11. Contract or Grant No.

13. Type of Report and Period Covered
Technical Note

12. Sponsoring Agency Name and Address
National Aeronautics and Space Administration
Washington, D. C. 20546

14. Sponsoring Agency Code

15. Supplementary Notes

16. Abstract
In situ measurements of the ambient concentrations of several atmospheric trace constituents were obtained using instruments installed on board the NASA Convair 990 aircraft at altitudes up to 12.5 kilometers over Alaska and the Arctic Ocean. As part of the NASA Global Atmospheric Sampling Program, concentration data on ozone, carbon monoxide, water vapor, and particles larger than 0.5 micrometer in diameter were acquired. Data were taken during three series of flights in April, August, and October of 1975.

17. Key Words (Suggested by Author(s))
Pollution monitoring
Global air pollution

18. Distribution Statement
Unclassified - unlimited
STAR category 45

19. Security Classif. (of this report)	20. Security Classif. (of this page)	21. No. of Pages	22. Price*
Unclassified	Unclassified	62	A04

* For sale by the National Technical Information Service, Springfield, Virginia 22161

IN SITU MEASUREMENTS OF ARCTIC ATMOSPHERIC TRACE CONSTITUENTS FROM AN AIRCRAFT

by Gregory M. Reck, Daniel Briehl, and Ted W. Nyland

Lewis Research Center

SUMMARY

In situ measurements of the ambient concentrations of several atmospheric trace constituents were obtained using instruments installed on board the NASA CV-990 aircraft at altitudes up to 12.5 kilometers. As part of the NASA Global Atmospheric Sampling Program, concentration data on ozone, carbon monoxide, water vapor, and particles larger than 0.5 micrometer in diameter were obtained. Data were taken during three series of flights in April, August, and October of 1975 over Alaska and the Arctic Ocean.

INTRODUCTION

As part of the NASA Global Atmospheric Sampling Program (GASP), atmospheric constituent data were obtained with the NASA CV-990 research aircraft during three series of flights in April, August, and October of 1975 over Alaska and the Arctic Ocean. GASP uses several commercial Boeing 747 airliners equipped with automated instrument systems to collect in situ measurements of several minor atmospheric constituents (refs. 1 to 3). The NASA CV-990 aircraft is used to evaluate sampling instruments and systems in flight (refs. 4 to 6) and to collect atmospheric data in regions that are not traversed by GASP-instrumented commercial aircraft.

The need for obtaining reliable data on the concentrations of a number of minor atmospheric constituents arises from the continuing concern regarding the potential effects of high-altitude aircraft exhaust emissions on the troposphere and lower stratosphere. In its' "Report of Findings" the Climatic Impact Assessment Program (ref. 7) emphasized the urgent need for detailed measurements of the natural composition of the upper atmosphere, as well as research and monitoring programs to obtain additional knowledge of the atmosphere and to detect changes in atmospheric quality. The global

distribution of minor constituents is necessary as an input to models of the upper atmosphere. Reference 7 suggests several important constituents in atmospheric investigations including ozone, carbon monoxide, water vapor, and airborne particles.

The objectives of the GASP experiment on the CV-990 were twofold: to extend the limits of the minor constituent data collected by GASP into the Arctic region and to provide flight evaluation data on several water-vapor instruments which were being developed for the automated monitoring systems. The GASP CV-990 installation included (1) an ultraviolet absorption ozone monitor, (2) a nondispersive infrared carbon monoxide monitor, (3) a light-scattering particle counter, (4) an aluminum oxide water-vapor monitor, and (5) a cooled-mirror, water-vapor monitor. The water-vapor monitors were flown as part of an effort to improve the water-vapor measurement and to evaluate instrument response. Due to the importance of water vapor in the atmosphere, a portion of the data from the water-vapor monitors is included to show qualitative trends.

The data presented in this report were obtained during three series of flights identified as the Arctic Experiment Program phases I, II, and III conducted during April, August, and October 1975, respectively. The three phases were coordinated by the NASA Ames Research Center and were conducted in conjunction with several other programs including the Arctic Ice Dynamics Experiment, The Bering Sea Mammal Experiment, the Polar Ice Studies, and others. Because GASP was not the principal experiment in any of the flights, data were gathered only for those flights or during those portions of flights when the aircraft was in a region of interest to the GASP researchers.

SAMPLING SYSTEM

A schematic diagram of the sampling system installed on the CV-990 is shown in figure 1. The sample flow for the ozone and carbon monoxide monitors was pressurized using a system similar to that described in reference 4. A single-stage diaphragm sample pump in combination with a back-pressure regulator maintained the sample pressure at 100 kilopascals. An absolute pressure regulator was used to supply the back-pressure regulator with a constant reference pressure to avoid variations in sample pressure that result from changes in cabin pressure. Each monitor's air sample flow was set at a constant value by adjusting its throttle valve downstream of the instrument. Rotometers upstream of the throttle valves were used to monitor the instrument flow rates. The advantages of operating the ozone and carbon monoxide monitors at higher than cabin pressure included a gain in instrument sensitivity and the elimination of leaks into the sample system from the cabin.

The ozone loss due to destruction in the sampling system was minimized by minimizing sample gas residence time in the system and by using ozone-compatible materials where possible. Ozone destruction tests conducted after phase III yielded the data shown

in figure 2. These tests included the inlet probe and inlet tubing as well as the pressurization system. The data indicate that the ozone lost in the sampling system was less than 12 percent of the incoming ozone concentration. All of the atmospheric ozone data presented in this report have been corrected for ozone destruction.

The sample flow for the particle monitor was not pressurized in order to avoid particle losses or contamination by a pump. A heat-transfer mass flowmeter located downstream of the instrument was used to measure sample flow rate. A vane pump in the instrument was used for several of the early flights to establish sample flow rate until it was determined that a fixed restriction downstream of the flowmeter maintained an acceptable flow rate throughout the altitude range of interest.

SAMPLING INSTRUMENTS

Ozone Monitor

Ozone measurements were made with a self-contained ultraviolet absorption photometer (described in ref. 8). The operation of this instrument was based on the measurement of the absorption by ozone at 253.7 nanometers in a 71-centimeter-long absorption chamber. Measurements were taken approximately every 20 seconds, on the completion of two half-cycle periods. During the first half cycle, the sample flow was passed through a catalytic ozone destruction filter (scrubber) to produce an integrated light intensity measurement. During the second half cycle the ozone was not scrubbed, and the light intensity was integrated over the same time period as the reference measurement. The difference between the two measurements was related to the ozone concentration.

The accuracy of the instrument was verified to within ±20 parts per billion by volume (ppbv) before phase I using the potassium iodide method and after phase III using an ozone generator calibrated by the potassium iodide method (ref. 9). The measurement precision of the instrument was ±5 ppbv. The instrument would respond to 90 percent of a step change in ozone concentration in approximately 30 seconds. Both zero and calibrate functions were provided on the instrument to check the instrument operation. Instrument flow rate was set at 3000 cubic centimeters per minute.

Carbon Monoxide Monitor

The carbon monoxide monitor was a single-beam, nondispersive, infrared, absorption analyzer using the dual-isotope fluorescence technique described in reference 10. This technique had the characteristic of a stable span calibration. The output of the car-

bon monoxide monitor was an analog signal of ±10 volts dc. The sensitivity of the monitor was measured as 152 ppbv per volt (±2 percent) using a flow dilution technique before phase II. Typical zero drift was approximately 20 ppbv per hour, thus it was necessary to periodically reset the zero by passing the sample flow through a heated catalytic filter that oxidized the carbon monoxide. In-flight zero checks required 10 minutes and were performed at approximately 30-minute intervals or as required. Because of a low-frequency random noise of ±20 ppbv, the output data were averaged over 5-minute intervals. The response characteristics of the instrument were primarily dependent on sample flow rate due to the large volume of the sample cell. With the flow rate of 5000 cubic centimeters per minute used during the flights, the instrument indicated 90 percent of a step change in carbon monoxide in approximately 3 minutes.

Light-Scattering Particle Counter

The particle counter used a forward light-scattering technique to measure the number of airborne particles over 0.5 micrometer in diameter. The operation was similar to that of the unit described in reference 11. As the air sample containing particles passed through the sensor, it was illuminated by a light beam, and light scattered by the particles in a forward direction was detected by a photomultiplier tube. Under normal operating conditions, each particle caused a pulse in the photomultiplier output. The particle concentration was determined by counting the number of output pulses during the counting period and then dividing that number by the corresponding sample volume during the same period, corrected to altitude ambient conditions. Particle counter volumetric flow rate was approximately 28 000 cubic centimeters per minute and the counting period was fixed at 1 minute.

During the laboratory evaluation of this instrument, it was found that the sample volume was not receiving uniform illumination. The sample volume illumination was mapped and a correction factor was developed by assuming a particle size distribution. The data and derivation of this factor are presented in the appendix. The correction factor has been applied to all of the data presented in this report. The accuracy of the correction factor is uncertain; however, the data have been included because relative changes in particle concentration observed by the instrument are believed to be valid.

Water-Vapor Monitors

Two measurement techniques were used at various times during the three flight series: an aluminum oxide (Al_2O_3) hygrometer and a cooled-mirror hygrometer. The Al_2O_3 hygrometer was used in all the flights; and the cooled-mirror hygrometer was

used for several phase II flights and for all phase III flights. Several mounting configurations of the Al_2O_3 hygrometer were flown as part of a developmental effort to improve the quality of the water-vapor measurement. The cooled-mirror hygrometer was being evaluated and compared with the Al_2O_3 instrument.

Aluminum oxide hygrometer. - This instrument consisted of two units: a sensing element (or sensor) and an electronics package. The sensing element consisted of a small strip of aluminum that was anodized to provide a porous oxide layer. A very thin coating of gold was evaporated over this structure. The aluminum base and the gold layer formed the two electrodes of a capacitor. The impedance of this capacitor varied with the amount of water absorbed into the porous surface. References 12 and 13 give further discussions of this technique.

Two mounting configurations of the sensing element are shown in figures 3(a) and 3(b). These configurations are similar to the mounting arrangements compared in reference 12. Each of the sensing elements was mounted in a commercially designed total-temperature airscoop adapted for the sensor. The primary difference between the configurations is the location of the sensing element: In figure 3(a) the sensor is located in a chamber below the airscoop, and the air sample is introduced into the chamber through a 0.32-centimeter-diameter tube; in figure 3(b) the sensor is located inside the hollow stem of the airscoop, which provides a higher ventilation rate than the chamber mount. The second configuration was expected to improve the sensor response rate.

The Al_2O_3 hygrometer calibrations supplied by the manufacturer were specified to be within $\pm 2\ C^o$ over the dew-frost point temperature (DFPT) range of 40^o to -65^o C and within $\pm 3\ C^o$ over the range -65^o to -110^o C. Each sensor was calibrated before and after each phase using the calibration system described in reference 2. The uncertainty of the DFPT calibration procedure is less than $\pm 2\ C^o$ over the range 0^o to -70^o C. The Al_2O_3 hygrometer water-vapor data presented in this report were obtained from sensors that repeated their calibrations within the uncertainty of the calibration procedure.

Since reference 14 indicated that the sensor calibration varied with the sensor temperature, each sensor was calibrated at several temperatures over the flight total-temperature range. A thermistor mounted beside the sensing element provided a temperature measurement with each data point. During the data reduction process, the temperature measurement was used to interpolate the DFPT from the family of calibration curves.

A correction factor was applied to the data obtained with the scoop-mounted sensors. The correction was necessary to compensate for the change in DFPT resulting from the ram pressure recovery. Wind-tunnel tests demonstrated that the recovery factor of the airscoop was nearly 1.

A serious concern with the application of the Al_2O_3 technique to aircraft measurements of water vapor was the response characteristics of the instrument to changes

in water vapor and ambient temperature. Response tests in the NASA calibration facility indicated that, at a constant ambient temperature of -40° C, the hygrometer required 15 to 30 minutes after a step change in water-vapor concentration to reach 63 percent of the difference between the initial and final values of DFPT. This result was in general agreement with the conclusions in reference 15.

Experiments conducted at Lewis indicate that the Al_2O_3 hygrometer responds to a decrease in ambient temperature as if it were a change in DFPT (see fig. 4). The Al_2O_3 hygrometer was placed inside a 65-cubic-centimeter housing, which was continuously purged with air. The DFPT of the purge air was constant at -49° C, as measured by a cooled-mirror hygrometer downstream of the Al_2O_3 hygrometer. The Al_2O_3 sensor, along with its housing, was placed inside an environmental chamber so that the ambient temperature of the sensor and the constant DFPT purge air could be reduced. As shown in figure 4, the ambient temperature was lowered from 26° to -40° C over a period of 45 minutes. With the ambient temperature at 26° C, the Al_2O_3 hygrometer agreed with the cooled-mirror hygrometer to within 1 C°. As soon as the ambient temperature of the purge air was reduced, the DFPT as measured by the Al_2O_3 hygrometer began to drop steeply, reaching a minimum of -77° C within 25 minutes after which the DFPT began to rise slowly. The Al_2O_3 hygrometer then took 170 minutes to indicate within 1 C° the correct DFPT. These experiments demonstrate that a change in static-air temperature at constant DFPT during flight will cause the Al_2O_3 hygrometer to indicate an erroneous DFPT until the hygrometer can reach equilibrium. The response time of the hygrometer is proportional to the rate and magnitude of the temperature change.

The most severe gradients in ambient temperature and water vapor are encountered as the aircraft climbs to cruise altitude, with ambient temperature and DFPT both decreasing. The response characteristics described in the preceding paragraphs suggest that the Al_2O_3 hygrometer would indicate too high a DFPT in response to the decreasing temperature. Thus, the possibility exists for compensating effects.

The recovery of the hygrometer from saturated conditions, as would be encountered with the passage of the aircraft through clouds, was very slow. The only available laboratory test data showed that, after having been subjected to saturated conditions for 40 minutes, the Al_2O_3 hygrometer continued to indicate saturation for 30 minutes after the air was no longer saturated. The test was terminated at this time, and no data are available for the time required for the Al_2O_3 hygrometer reading to return to the true DFPT.

In spite of its stated limitations, it is felt that the water-vapor measurements obtained with the Al_2O_3 hygrometer are of interest and they are reported when available. Because of the uncertainty of the time constant, no correction has been applied to the data to compensate for the response characteristics.

Cooled-mirror hygrometer. - This instrument also consisted of two units: a sensing

unit and an electronics package. The sensing unit consisted of a mirror mounted on a two-stage thermoelectric cooler. The sample flow was directed across the face of the mirror. The mirror is illuminated, and two photodetectors are located so as to monitor the direct and diffuse components of the reflected light. The photodetectors are arranged in a bridge circuit. In operation, the mirror is cooled until a thin condensate layer is maintained on the mirror surface and the output of the optical bridge is balanced. This point is the dew-frost point temperature and was measured by a platinum resistance thermometer. The sensor unit was mounted below an airscoop, which was identical to the airscoop used for the Al_2O_3 hygrometer. A sketch of the mount is shown in figure 3(c).

The range of the cooled-mirror hygrometer was limited by the temperature depression capability of the thermoelectric cooler, which in turn was limited by the temperature of the heat sink to which the cooler was attached. The aircraft skin was used as the heat sink. Figure 5 shows the minimum or lowest DFPT that could be measured by the hygrometer at flight Mach 0.82. The accuracy of the measurement depended on the accuracy of the mirror temperature measurement, which was $\pm 0.6\ C^{o}$. Figure 5 represents the theoretical cooling capability of the hygrometer, which will be reached only if there is a perfect path between the hot junction of the thermoelectric cooler and the aircraft skin. The response rate of the instrument to changes in water-vapor concentration was primarily dependent on the cooling rate of the thermoelectric cooler, which was $0.12\ C^{o}$ per second.

INSTALLATION

The GASP sampling equipment was installed aboard the NASA CV-990 research aircraft based at the Ames Research Center, Moffett Field, California. The CV-990 is a four-engine jet passenger aircraft, which has been modified with special viewing ports, power supplies, instrumentation, computing systems, and other general use facilities to accommodate a wide variety of airborne research programs (ref. 16).

The stainless-steel sample inlet and static discharge probes were assembled as shown in figure 6(a) and installed in a passenger window frame in the forward part of the aircraft as shown in figure 6(b). The sample inlet probe penetrated the aircraft skin enough to avoid ingestion of boundary-layer air. Isolation ball valves and bypass line permitted purging of the inlet probe with ambient air when measurements were not being taken.

The airscoops containing the hygrometer sensing elements were each mounted on a standoff pedestal to avoid ingestion of boundary-layer air. Two of these hygrometer scoop assemblies were mounted side-by-side on a blank plate and installed in a zenith port (fig. 6(c)). Total-pressure probes mounted on an identical airscoop and flown on a checkout flight verified that the airscoop inlet was outside the boundary layer of the air-

craft. The water-vapor sensor assemblies could be interchanged between flights to permit comparisons of the various hygrometer configurations.

The remainder of the sampling equipment was installed in two equipment racks designed for use aboard the CV-990 aircraft. Photographs of the installation are shown in figure 7. The equipment rack on the starboard side of the aircraft was less than 50 centimeters aft of the window that contained the sample probe assembly. The two equipment racks were located opposite each other across the aisle. Sample tubing connecting the racks was routed across the aisle at floor level.

The output data from each of the sampling instruments and from the transducers in the flow system were recorded on the Aircraft Digital Data Acquisition System (ADDAS) at 1-second intervals during the flights. In addition, the analog output signals from several instruments were recorded on two strip-chart recorders located in the GASP equipment racks. The output from the particle counter was recorded on a digital printer after each count cycle. A Greenwich mean time (GMT) time code signal was recorded on the strip charts, the printer, and the ADDAS data record for correlation of flight events. The aircraft location (latitude, longitude, and pressure altitude) and flight parameters (static-air temperature, wind speed, wind direction, air speed, pitch, roll, etc.) were also recorded on the ADDAS data record. The aircraft's inertial navigation system determined its position. An onboard computer performed some data conversions and displayed this information along with selected flight parameters on an onboard line printer at 20-second intervals for real-time data evaluation.

FLIGHT ROUTES

A summary of the origin and destination of each of the flights in the three phases of the program is given in table I. This report presents data from only a portion of those flights, as indicated in the table. The high-altitude portions of the flight routes from which data are presented are shown in figure 8. Where several flights were made along the same general route, the individual flights are not shown.

The flight routes fall into four general categories: (1) polar flights, (2) ice camp flights, (3) marine survey flights, and (4) ferry flights. The polar flights (phase I, flights 11 to 13) were particularly useful for air sampling since they were long, high-altitude flights. The ice camp flights (phase I, flights 10 and 14 to 17; phase II, flights 4, 6, and 9; and phase III, flights 3, 6, 8, 9, and 12) were useful because they yielded repetitive data along the same route. Each of these flights consisted of a high-altitude outbound segment to a group of ice camps located in the Beaufort Sea, a pattern of runs at varying altitudes over the camps, and a high-altitude inbound segment. Each of the marine survey flights (phase I, flights 4 to 7; phase II, flight 5, 7, 8, and 10; and

phase III, flights 4, 5, 7, 10, 11, and 13) consisted of a high-altitude outbound segment, a low-altitude survey, and a high-altitude inbound segment. The high-altitude segments of most of the marine survey flights were so short that data from those flights have been omitted. Of the various marine survey flights only data from flights 5, 6, and 7 of phase I are reported. The ferry flights (phase I, flights 3, 8, 9, and 18; phase II, flights 3 and 11; and phase III, flights 2 and 14) were high-altitude flights between Moffett Field and Alaska.

RESULTS AND DISCUSSION

The atmospheric constituent data obtained on the CV-990 during the AEP are shown in figures 9 to 18. For each flight indicated in table I, a separate figure, which contains all data acquired during the flight, is presented. The data are presented in this manner to depict the relationship and variation among the constituents as the aircraft encountered and crossed atmospheric features. These data should be useful in examining the behavior of the constituents during specific events as well as in evaluating average constituent levels.

For convenience in discussing the results, the data have been grouped according to the types of flights (polar, ice camp, marine survey, and ferry). The atmospheric constituent data shown in figures 9 to 18 have been presented as discrete data points obtained at 5-minute intervals. This frequency is consistent with the rate of data acquisition on the GASP-equipped Boeing 747 systems. Lines have been drawn connecting the data points to aid in evaluating the data. The flight parameter data curves shown in the figures (altitude, static-air temperature) were drawn from data obtained at 1-minute intervals. The flight altitude data shown in the figures were obtained from the aircraft altimeter which measured pressure altitude, rather than geometric altitude. The wind barbs are shown at 10-minute (or longer) intervals and follow standard National Weather Service (NWS) plotting convections. All of the data shown in the figures have been plotted as a function of time (GMT). To aid in obtaining the physical location of the data, latitude and longitude coordinates have been included at several points for each flight. A number of Al_2O_3 sensor elements were used during the flights, and each sensor was assigned a different plotting symbol which was used consistently throughout the data figures. At the beginning of each of the subsequent flight discussions, the figure containing the flight data is identified in parenthesis immediately after the flight number.

Phase I: Polar Flights

Data from the three flights in the polar series flown during phase I are shown in fig-

ure 9. The aircraft penetrated the tropopause (altitude, ~10 km) on all three flights. The tropopause encounters were apparent from minima in the static-air temperature data as well as changes in the measured constituents. The changes in ozone varied from typical values of less than 100 ppbv below the tropopause to 400 to 950 ppbv above. Carbon monoxide concentration data also showed good correlation with the tropopause, changing from values generally greater than 100 ppbv below to values generally less than 50 ppbv above the tropopause. The DFPT data from both Al_2O_3 hygrometers indicated drier air above the tropopause. In many cases, the hygrometers showed good agreement; where they did not, the chamber-mounted sensor generally showed drier air than the scoop-mounted sensor. The DFPT data are shown in the figures even where higher than the static-air temperature to show sensor response characteristics. Light-scattering particle concentration data did not vary greatly across the tropopause, although particle concentrations in the stratosphere were more steady with time than in the troposphere.

Flight 11 (fig. 9(a)). - The first polar flight on April 16, 1975, penetrated the tropopause during climbout and remained in the lower stratosphere until final descent. There is an indication from the static-air temperature of a depression in the tropopause which the aircraft passed over at approximately 1730 GMT. Both the ozone concentration and the static-air temperature had been increasing before that time, and the ozone reached a maximum value of 950 ppbv. The ozone concentration continued to vary from 400 to 700 ppbv throughout the remainder of the flight. The aircraft crossed the north pole at 1855 GMT at an altitude of 10.5 kilometers.

Flight 12 (fig. 9(b)). - The second flight in the polar series on April 17, 1975, ranged over central and southern Greenland at an altitude of 10.0 kilometers. The variations in the static-air temperature indicate several penetrations of the tropopause. After initially crossing the tropopause during climbout, the aircraft slowly crossed back into the troposphere at approximately 1650 GMT. This encounter occurred at a constant flight altitude indicating an upward sloping tropopause along the flight path. Later in the flight, variations in static-air temperature, ozone, and carbon monoxide concentrations indicated air of stratospheric origin. The ozone concentration did not return to the values initially observed in the stratosphere (approximately 600 ppbv) until 1945 GMT when the aircraft was near 72° N latitude. Similar behavior was observed in the carbon monoxide concentration and static-air temperature.

Flight 13 (fig. 9(c)). - The third flight in the series on April 19, 1975, again crossed directly over the North Pole, this time at an altitude of 10.0 kilometers (approximately 0.5 km below the first crossing during flight 11). The ozone concentration data were approximately 100 ppbv less than the data recorded during the first flight, although the static-air temperature recorded over the pole was the same for both flights at -49° C. The aircraft apparently encountered the tropopause at a slant angle near 1700 GMT; however, the climb from 8.5 to 10.0 kilometers at 1715 GMT masked this

effect. The static-air temperature showed little variation in the stratosphere and the increase to -41° C observed at 79° N during the first flight did not reoccur. A climb from 10.0 to 10.5 kilometers at 1924 GMT caused little effect on any of the measured parameters. The static-air temperature began to decrease at 2015 GMT, indicating that the aircraft was approaching the tropopause, and the crossing occurred when the aircraft descended to 10.0 kilometers at 2051 GMT. Later in the flight, several ozone peaks occurred which correlated with decreases in carbon monoxide concentration, indicating brief encounters with stratospheric air.

Phase I: Ice Camp Flights

Data from the five ice camp flights flown during phase I are shown in figure 10. The aircraft penetrated the tropopause on every flight, usually on both the outbound and inbound segments of the flights. The tropopause height was approximately 10 kilometers throughout the flights. Variations in ozone, carbon monoxide, and water-vapor concentrations as the aircraft crossed the tropopause correlated as expected. Stratospheric ozone concentrations were typically in excess of 400 ppbv and as high as 850 ppbv. Carbon monoxide concentrations were typically less than 50 ppbv in the stratosphere. Agreement between the two Al_2O_3 hygrometers deteriorated during these flights, but generally showed near-saturated conditions in the troposphere and dry conditions in the stratosphere. Stratospheric DFPT ranged from 10 to 20 C° colder than the static-air temperature. The particle concentration data showed some structure, and on several occasions peaks were observed near the tropopause. The particle concentration data showed little variability in the stratosphere.

Flight 10 (fig. 10(a)). - The first of the ice camp flights on April 10, 1975, encountered a perturbation from a flat tropopause as the aircraft completed its climbout at 10.7 kilometers. The static-air temperature dropped to -59° C and the ozone and carbon monoxide concentration data began to indicate stratospheric air. However, within 5 minutes the air temperature again began to decrease and eventually reached a minimum value of -61° C. Both the ozone and carbon monoxide data returned to tropospheric values. Subsequently, the static-air temperature began to increase and the constituent data indicated stratospheric air. The aircraft reached the vicinity of the ice camps at 2020 GMT and began a survey pattern at the same flight altitude. The pattern was completed at a lower altitude, and the aircraft then climbed to 8.8 kilometers for the inbound segment. A brief encounter with stratospheric air indicated a tropopause height of less than 10 kilometers at 75° N.

The stratospheric ozone concentrations recorded on flight 10 were higher than on subsequent ice camp flights. Ozone concentrations during the outbound segment sometimes exceeded 800 ppbv. However, these values are consistent with the ozone concen-

trations measured on the first polar flight (flight 11), which occurred two days after flight 10.

The particle concentration data in the stratosphere from flight 10 were higher than most of the particle data acquired on the polar flights. The peaks observed during the inbound segment after 2350 GMT were likely due to intermittent cirrus clouds observed at the flight altitude. Reference 6 demonstrates that the particle counter is sensitive to the presence of clouds. Two peaks in the particle concentration data were observed in the stratosphere during the outbound leg; however, no explanation is apparent.

Flights 14 and 15 (figs. 10(b) and (c)). - The second and third of the ice camp flights, both on April 21 and 22, 1975, were similar in terms of the flight profile and the constituent data. The tropopause was encountered on both flights as the aircraft climbed from 9.4 to 10.7 kilometers, and the tropopause temperatures were near -59° C. The ozone concentrations measured in the stratosphere over the ice camps were approximately 600 ppbv and showed less fine structure in the horizontal profile than on earlier flights. Peaks in the particle concentration data were observed on both flights during the outbound segment while the aircraft was just below the tropopause. However, once the aircraft entered the stratosphere, the particle concentration data became constant and showed much less variability than tropospheric particle data. Very thin cirrus clouds were observed to the sides of the aircraft during flight 14 at 2012 GMT. No clouds were observed at flight level on flight 15, although a dense cloud deck was observed below the aircraft. The tropospheric DFPT data for both outbound flight segments were near saturation values. The cloud observations and the presence of a contrail behind the CV-990 both support the water-vapor data.

The aircraft crossed the tropopause again on the inbound segment of both flights during the climbout from the final low-altitude pattern. The inbound segments were at an altitude of 10.7 kilometers. The lower ozone concentrations observed on flight 14 suggested that flight 14 was closer to the tropopause than flight 15. The two Al_2O_3 hygrometers showed poor agreement during the inbound segments. The scoop-mounted sensor indicated near-saturated DFPT values, while the chamber-mounted sensor gave DFPT values 10° to 15° C colder than the static-air temperature and showed better agreement with the data obtained on the outbound segment. The lack of agreement between the sensors may have been a result of differences in sensor recovery from the wet conditions encountered in clouds during the lower altitude segments.

Flight 16 (fig. 10(d)). - Only two short segments of the fourth flight of this series on April 24, 1975, were sufficiently high to encounter the tropopause. The tropopause was crossed during the outbound segment at an altitude of 9.4 kilometers. The tropopause temperature was observed to be -58° C. Shortly after the crossing the aircraft climbed to 10.7 kilometers and then descended for a segment at 4.6 kilometers. During the brief period at 10.7 kilometers, the ozone concentration reached 600 ppbv, which

agreed with the values observed on flights 14 and 15. A sharp peak was observed in the particle concentration data just before the tropopause was crossed. No clouds were observed although a thick haze was visible on both sides of the aircraft.

The tropopause was crossed a second time during the climbout for the inbound segment. The aircraft remained in the stratosphere throughout the inbound cruise at an altitude of 10.7 kilometers until the aircraft began its final descent. The hygrometers continued to disagree, with the chamber-mounted sensor yielding lower DFPT than the scoop-mounted sensor. Both sensors appeared to respond very slowly to the stratospheric conditions.

Flight 17 (fig. 10(e)). - The final flight of this series on April 26, 1975, was similar to the earlier flights in that both the outbound and the inbound segments were in the stratosphere at 10.7 kilometers. Ozone and carbon monoxide values were comparable with earlier flights, and the poor agreement between the DFPT data from the chamber-mounted and scoop-mounted sensors persisted.

An interesting feature appeared during the initial climbout and cruise segment at an altitude of 9.4 kilometers. The ozone and carbon monoxide data indicated an apparent depression in the tropopause, which the aircraft passed through before it ultimately crossed into the stratosphere during a climb to 10.7 kilometers. The constituent concentration levels observed in the depression were comparable with stratospheric levels measured at 10.7 kilometers and farther north (75^{o} N).

Phase I: Marine Survey Flights

Data from three of the marine survey flights flown on consecutive days during phase I are shown in figure 11. Each of these flights consisted of an initial high-altitude outbound segment and a high-altitude inbound segment over the same route. These segments were separated on each flight by a low-altitude survey, during which the pressurized sampling system was turned off. Good correlation was observed between carbon monoxide and ozone measurements as the aircraft crossed the tropopause.

Flight 5 (fig. 11(a)). - The tropopause was encountered on both segments of this April 6, 1975, flight. A dramatic increase in ozone and decrease in carbon monoxide were observed during the climb from 8 to 12 kilometers altitude at 0055 GMT.

Flight 6 (fig. 11(b)). - The tropopause was again encountered on April 7, 1975, on both high-altitude segments of this flight. High values of ozone mixing ratio, in excess of 1200 ppbv were obtained at 12 kilometers altitude on the inbound segment. The Al_2O_3 hygrometer indicated very dry conditions in the stratosphere.

Flight 7 (fig. 11(c)). - High values of ozone, indicative of stratospheric air, were observed on the outbound segment of this flight on April 8, 1975; however, the stratosphere was apparently encountered on a slant angle since the ozone data gradually increased to

the 700-ppbv level. A reduction in ozone level from the peak value at 2040 GMT was coincident with a change in wind direction at a level flight altitude of 10.5 kilometers. A more dramatic example of the effect of the shift in wind direction occurred during the inbound segment at an altitude of 9 kilometers. A gradual increase in ozone concentration with corresponding decreases in carbon monoxide and water vapor were observed until 0030 GMT, when the wind direction changed and constituent concentrations typical of tropospheric air were observed.

Phase I: Ferry Flights

There were four ferry flights during phase I, two between Moffett Field and Anchorage for the marine survey series, and two between Moffett Field and Fairbanks for the polar and ice camp series. Data obtained from these flights are shown in figure 12. Flights 3 and 8 to and from Anchorage followed routes over the Pacific Ocean and the Gulf of Alaska. Flights 9 and 18 to and from Fairbanks followed a more direct flight route which remained closer to the coastline.

Flight 3 (fig. 12(a)). - This flight on March 31, 1975, passed directly over a weathership station located at 50° N and 145° W. Interruptions in the data record resulted in a loss of data for early portions of the flight. The scattered data available indicate that large variations in the constituent concentrations may have been occurring at approximately 1810 GMT when the aircraft passed into a high-velocity wind stream. At approximately 2200 GMT, changes in the carbon monoxide and DFPT did occur as the direction of the high-speed winds changed. DFPT data after 2210 GMT indicated dry air, but the increase in carbon monoxide indicates that the air was not of stratospheric origin. Thin cirrus clouds were noted at flight altitude between 2030 and 2200 GMT, where the Al_2O_3 hygrometer indicated saturated air.

Flight 8 (fig. 12(b)). - This ferry flight on April 9, 1975, took a more direct route between Anchorage and Moffett Field than flight 3. The aircraft penetrated the tropopause during climbout and remained in the stratosphere until 1940 GMT. At this time the ozone concentration decreased abruptly as the aircraft again passed through the tropopause. The decrease in ozone on this occasion was more rapid than on previous encounters with the tropopause at constant flight altitude, which suggested a rapid increase in the tropopause height along the flight route.

Flight 9 (fig. 12(c)). - On this flight on April 12, 1975, most of the climb data before 1840 GMT were not recorded by the computer. Between 1830 and 1950 GMT the data indicated tropospheric air At approximately 1950 GMT an increase in ozone coincided with a peak in wind speed, and the temperature, carbon monoxide, and water vapor all indicated passage into stratospheric air. Particulate data showed very little variability during this period although the ozone concentration varied from 200 to almost 500 ppbv.

Flight 18 (fig. 12(d)). - The early portion of this ferry flight (before 2000 GMT) on April 27, 1975, indicated occasional penetrations into stratospheric air represented by the ozone peaks (300 ppbv) that rose above the tropospheric ozone levels of 50 to 100 ppbv. Although carbon monoxide data were not available until after 1930 GMT, the first 30 minutes of data showed variability between 115 and 210 ppbv. The aircraft crossed the tropopause during the climb at 2000 GMT and remained in the stratosphere until after 2200 GMT. At 2200 the wind speed began to increase, and the air temperature began to decrease. As the wind speed reached a maximum value of 95 knots, the ozone had diminished to less than 100 ppbv, and the air temperature had decreased to -60° C. Shortly thereafter the aircraft began its descent.

Phase II: Ice Camp Flights

Data from the three ice camp flights of phase II in August 1975 are shown in figure 13. The tropopause was again encountered on all flights; however, the measured ozone concentration values were smaller than those observed during the phase I flights in April. The carbon monoxide concentrations in the stratosphere were similar to levels observed earlier in the year. Tropospheric DFPT were near saturation and clouds were frequently encountered at altitudes below 10 kilometers. Data from the optical particle counter indicated generally lower particle concentrations than during phase I.

Flight 4 (fig. 13(a)). - Several peaks in ozone concentration were observed during the early portions of this flight on August 18, 1975 (at 2100 and 2235 GMT); however, the data did not indicate a stratospheric penetration until the inbound segment of the flight at 0100 GMT, when the aircraft climbed to 12.5 kilometers. At this point, carbon monoxide concentrations and the DFPT decreased, as expected, in the stratosphere. On this flight, two Al_2O_3 scoop-mounted sensors were flown. No explanation is apparent for the differences in DFPT data between the sensors.

Flight 6 (fig. 13(b)). - This flight on August 22, 1975, was similar to other ice camp flights in that the flight plan included a number of parallel lateral traverses of a triangular area over the ice camps at a constant flight altitude of 10.7 kilometers. The pattern was particularly interesting on this date since it was apparent that the tropopause crossed through the triangle at the flight altitude on a slant angle. Thus, the constituent data (fig. 13(b)) taken between 2100 and 0010 GMT indicate a cyclic pattern which resulted from periodically crossing the tropopause. The inverse correlation between ozone and carbon monoxide concentration data is apparent. The DFPT data from the scoop-mounted sensor also correlate with the carbon monoxide data; however, data from the chamber-mounted sensor remains saturated throughout the flight. The data from the optical particle counter indicate a slightly larger particle concentration in the stratosphere than in the troposphere.

The pattern over the camps consisted of a flight leg along the base of the triangle followed by 5 parallel legs each offset from the previous leg by about 1.6 kilometers. Upon reaching the apex of the triangle, the aircraft executed a 360^{o} turn and retraced the pattern. The maneuver took approximately 3 hours, during which the wind remained relatively steady at 50 ± 10 knots from 280^{o}.

Air temperature data acquired during the pattern are shown in figure 14 in the form of isotherms superimposed on the flight route. Since the local situation changed considerably during the $1\frac{1}{2}$ hours required to traverse the triangle once, the data for the initial and final runs have been plotted separately. The minimum temperature recorded during the traverses was -60^{o} C, which agrees with the NWS tropopause temperature observation of -59.5^{o} C at Point Barrow, Alaska, at 0000 GMT on August 23, 1975. In addition, the NWS reported a tropopause height of 234 hectopascals (millibars) or 10.9 kilometers, which agrees well with the flight altitude. The data indicate a drift in the isotherms along the wind direction during the 3-hour period.

The ozone and carbon monoxide data are shown in figure 15. The ozone data are presented as isopleths of constant mixing ratio. The ozone isopleths have the same general shape as the isotherms, except for the final runs where the isotherms are bending sharply to the north. Also on the final set of runs, maximum ozone concentrations were observed across the middle of the pattern (between the two 300 ppbv isopleths shown). Carbon monoxide data are shown at the positions along the flight route where the data were acquired. Carbon monoxide levels are lower for the final runs, which condition is consistent with the warmer air temperatures and indicates stratospheric air. The carbon monoxide concentration increases as ozone concentration decreases and the lowest values are consistent with the observations of stratospheric carbon monoxide of reference 17.

Flight 9 (fig. 13(c)). - A triangular mosaic pattern similar to that flown on flight 6 was repeated on August 27, 1975; however, the aircraft descended from 10.5 to 8.5 kilometers for the pattern. The static-air temperature data shown in figure 13(c) indicate that the initial and final segments of the flight were well into the stratosphere, but the pattern was flown in the troposphere. During the mosaic pattern, a thin cirrus cloud deck was observed just below flight level. Ozone and carbon monoxide data indicated tropospheric values and the hygrometer remained saturated during the pattern. The particle concentration data indicated significantly smaller values during the initial and final flight segments in the stratosphere than during the pattern segment in the troposphere. However, the changes in concentration did not coincide with the tropopause penetrations, but appeared to be related to the changes in the wind speed and direction.

Phase II: Ferry Flights

The two phase II ferry flights between Moffett Field and Fairbanks followed nearly

the same routes, both passing over the weathership located at 50° N and 145° W. The data obtained from these flights are shown in figure 16. Ozone concentration values did not exceed 400 ppbv, and large variations in constituents were generally coincident with high-speed winds.

Flight 3 (fig. 16(a)). - During the early portion (before 2200 GMT) of this flight on August 15, 1975, the data indicated tropospheric air. Air temperature data were not available until 2030 GMT; however, ozone concentrations were small and carbon monoxide levels were typical of tropospheric air. The DFPT data indicated saturated or near-saturated air, which agreed with observations of intermittent, thin cirrus clouds at flight level and the presence of a contrail behind the aircraft. The intermittent clouds were also apparent in the sporadic peaks in particle concentration. At 2200 GMT the aircraft entered a region of stratospheric air that was split by a high-speed stream of air at 2230 GMT. Nearly all constituent data indicated the stream to be of tropospheric origin. Subsequently, all constituents returned to their former levels until the initial descent at 2300 GMT.

Flight 11 (fig. 16(b)). - The initial segment of this flight on August 29, 1975, appears to have remained in the troposphere; however, at approximately 2100 GMT both carbon monoxide and DFPT indicated the possibility of stratospheric air. Subsequent ozone data supported this observation. A shift in wind direction at approximately 2220 GMT interrupted the stratospheric indication briefly.

During the initial segment of this flight, DFPT data were obtained with the cooled-mirror hygrometer in addition to the Al_2O_3 hygrometer. The agreement between the hygrometers was good; however, an iceplug developed in the mirror hygrometer sample tube during climbout at 2020 GMT, and no further data were acquired until final descent.

Phase III: Ice Camp Flights

Data from the five ice camp flights of phase III in October 1975 are shown in figure 17. The tropopause was again encountered on all flights; however, as in phase II, the measured ozone concentrations were smaller than those observed during phase I in April. Stratospheric concentrations of carbon monoxide were similar to those obtained during phases I and II. The DFPT data generally indicated saturated air at flight levels below the tropopause. Particle counter data indicated generally lower particle concentration than on either phase I or phase II.

Flight 3 (fig. 17(a)). - On this flight, on October 10, 1975, penetration into the stratosphere occurred early during the outbound leg and continued until the aircraft descended for a low level run at 2300 GMT. Unusually constant ozone concentrations of about 300 ppbv were recorded for about 3 hours between the initial stratospheric penetration and the end of the run at 9.5 kilometers altitude. During this time, the particle

concentration was quite constant. An Al_2O_3 hygrometer with a scoop-mounted sensor was used during this series along with the cooled-mirror hygrometer. During the first stratospheric penetration of this flight, the Al_2O_3 hygrometer indicated a relatively constant DFPT. The DFPT as measured by the cooled-mirror hygrometer was several degrees higher than the Al_2O_3 hygrometer, indicating that the cooled-mirror hygrometer may have reached the limit of its cooling capacity. Figure 5 shows that at a static-air temperature of -48° C, the lowest DFPT capability of the cooled-mirror hygrometer is -63° C, which is 7 C° below the lowest DFPT measured by the hygrometer during the flight. The cooled-mirror hygrometer was not able to reach its minimum DFPT capability probably because a good thermal path did not exist between the aircraft skin and the hot junction of the thermoelectric cooler. A second stratospheric penetration occurred on the return leg at an altitude of 12.5 kilometers. The wind direction at this altitude was shifted about 90° from the wind direction at the 9.5-kilometer run. Ozone concentration peaked at a higher value than was reached during the 9.5-kilometer run, but the concentration was more variable.

Flight 6 (fig. 17(b)). - A brief stratospheric penetration starting at 1930 GMT occurred on October 15, 1975, during the outbound leg at 9.5 kilometers. During this period the ozone concentration peaked at about 200 ppbv, and the Al_2O_3 hygrometer briefly indicated unsaturated conditions. The wind velocity decreased. On the return leg of the flight at 12.5 kilometers, stratospheric conditions were again encountered as indicated by the rise in static-air temperature, higher ozone concentrations, and a drop in the DFPT on the Al_2O_3 hygrometer. For the rest of the flight, ozone and carbon monoxide showed tropospheric conditions, and the Al_2O_3 hygrometer was saturated. Data from the particle counter displayed a cyclic pattern during the traverses over the ice camps which may have been caused by the aircraft encountering different air masses.

Flight 8 (fig. 17(c)). - On October 20, 1975, penetration into the stratosphere occurred at 2200 GMT when the aircraft climbed from 9.5 to 10 kilometers. The Al_2O_3 hygrometer then began to display unsaturated conditions, and the ozone concentration began to rise. When the aircraft climbed from 10 to 10.5 kilometers, ozone concentrations increased, and the Al_2O_3 hygrometer began to indicate drier air. Particle counter data indicated slightly lower particle concentration after penetration into the stratosphere. Wind direction and speed remained relatively steady during the flight. The cooled-mirror hygrometer DFPT was several degrees higher than that indicated by the Al_2O_3 hygrometer and indicated frost points above saturation for most of the flight. The purpose of this flight was to make radar runs off the northern coast of Alaska. It is included with the ice camp flights because of its relatively long duration at high altitude.

Flight 9 (fig. 17(d)). - On October 22, 1975, after a low-level run along the northern coast of Alaska, the flight continued at 11.5 kilometers to the ice camps. A peak in the particle density at 2210 GMT, encountered during the climb to 11.5 kilometers, was caused by flight through dense clouds. The stratosphere was encountered during the

climb as indicated by the rise in static-air temperature. Ozone concentration increased to high levels, and the Al_2O_3 hygrometer indicated unsaturated conditions. The latter part of the flight was flown at 12.5 kilometers. A drop in the ozone concentration at 0020 GMT corresponded to slight change in wind direction.

Flight 12 (fig. 17(e)). - This flight on October 26, 1975, was flown at an altitude of 9.5 kilometers except for the return leg. Penetration into the stratosphere occurred at 2025 GMT as indicated by the rise in static-air temperature and the lowering of the DFPT as indicated by the Al_2O_3 hygrometer. At this time there was a mild rise in the ozone concentration accompanied by a shift in the wind direction. Tropospheric air was again encountered from 2330 to 0025 GMT. During this time the hygrometer again indicated saturated conditions, and the ozone concentration fell by about 25 percent. The return leg was flown in the stratosphere at 12.5 kilometers. Carbon monoxide concentrations achieved low values typically found in the stratosphere only during the last portion of the flight.

Phase III: Ferry Flights

Flight 2 (fig. 18(a)). - Only ozone and particle concentration data were obtained for this flight on October 8, 1975. The altitude for this flight was a constant 9.5 kilometers. Particle concentrations indicated the presence of clouds during the initial portion of the flight until 1900 GMT. It is not clear from the static-air temperature whether there was a penetration into the stratosphere, although there were several ozone peaks of 200 ppbv. A wind direction shift of nearly 180° at 1950 GMT did not correspond to any noticeable change in either ozone or particle concentration.

Flight 14 (fig. 18(b)). - On October 29, 1975, there was an initial climb to 9.5 kilometers followed by a low-level run along the Alaskan coast. Penetration into the stratosphere occurred during the initial 9.5-kilometer run as indicated by the ozone peak at 1935 GMT. An encounter with the jet stream was made when the aircraft again climbed to 9.5 kilometers. Wind speeds were high, and their direction gradually changed 90° from west to north during the period from 2040 to 2310 GMT as the aircraft flew south. Beginning at 2250 GMT, the ozone concentration increased to stratospheric levels, and the Al_2O_3 hygrometer became unsaturated and remained so until the end of the flight. At 2320 GMT the wind direction abruptly shifted from north to southwest and the speed dropped from 35 to 10 knots. The ozone concentration decreased somewhat after this wind direction shift. Wind speed then steadily increased until it reached 120 knots at the end of the flight. Carbon monoxide remained at tropospheric levels throughout the flight. Particle concentrations were highly variable during the flight at 9.5 kilometers. The lowest reading of the entire flight series was recorded at 2200 GMT.

SUMMARY OF RESULTS

In situ measurements of the ambient concentrations of several atmospheric trace constituents were obtained from the NASA Convair 990 aircraft at altitudes up to 12.5 kilometers over Alaska and the Arctic Ocean. Concentration data were taken during three series of flights in April, August, and October of 1975. The following were the results:

1. Carbon monoxide and ozone concentrations correlated well with static-air temperature changes that indicate penetration into the stratosphere. Carbon monoxide concentrations in the troposphere ranged from 50 to 200 ppbv and in the stratosphere were generally below 50 ppbv. Concentrations of ozone were generally below 100 ppbv in the troposphere and ranged up to 1200 ppbv in the stratosphere.

2. The light-scattering particle concentration data showed very little variation during flight in the stratosphere compared with flight in the troposphere. The relatively constant-valued particle data correlated well with other stratospheric indicators except on one flight when a change in stratospheric particle concentration coincided with a change in wind speed and direction.

3. The highest ozone concentrations were measured in April, which is consistent with the expected seasonal variation in ozone concentrations. Light-scattering particle concentrations in the stratosphere were highest during phase I and successively lower during phases II and III. Stratospheric carbon monoxide data were relatively constant throughout the three phases.

4. Water vapor generally correlated with stratospheric penetration, that is, the sensors tended to indicate drier air as soon as the stratosphere was encountered. However, long sensor response times and sensitivity to temperature changes as well as water vapor precluded critical observations of DFPT. Data from a cooled-mirror hygrometer showed good agreement with data from an Al_2O_3 hygrometer during a portion of one flight; however, the cooled-mirror hygrometer was apparently unable to reach extremely low stratospheric frost points due to a limited temperature depression capability.

5. On one occasion, a pattern consisting of a series of parallel runs at constant altitude was flown which, fortuitously, coincided with the local tropopause. Ozone concentration data acquired as the aircraft repeatedly crossed the region were sufficiently repeatable to permit isopleths of constant ozone mixing ratio to be drawn. The ozone isopleths compared favorably with isotherms across the pattern, and carbon monoxide data were consistent with the ozone and temperature data.

Lewis Research Center,
National Aeronautics and Space Administration,
Cleveland, Ohio, February 15, 1977,
197-10.

APPENDIX - PARTICLE COUNTER CORRECTION FACTOR

A count correction factor was developed to overcome the illumination problems associated with this instrument. The error stems from the facts that the illuminated volume is not as large as the sample nozzle cross-sectional area and that the area is not uniformly illuminated. As a result not all particles are counted, and the actual number that are counted are dependent on their size. The dependence on size means that a simple correction factor is not sufficient and that an assumed particle density distribution must be used to establish a count correction factor.

Effect of nonuniform illumination. - A particle passing through the illuminated volume within the instrument scatters light, the amounts of light scattered being a function of the particle diameter and the intensity of illumination. The scattered light is converted by a photomultiplier tube to a voltage pulse. Through calibration, a curve of voltage pulse height as a function of particle diameter for constant illumination is obtained and is shown in figure 19.

To obtain the number of particles greater than 0.5 micrometer, a voltage pulse height discriminator is adjusted to 0.07 volt (see fig. 19) so that only pulses equal to or greater than this level will be counted as particles.

If a particle passes through the illuminated volume where the intensity is less than that for which the calibration curve applies, it may or may not get counted, depending on its size and the relative intensity of illumination along the particle flow path. Measurements were made to determine the relative light intensity throughout the illuminated volume. A 0.12-millimeter-diameter optical fiber was used as a probe with a silicon photodiode as a detector. Figure 20 shows the results of these measurements. The four curves are for measurements taken in the interval $-1 < y < +1$ millimeter. Also shown in the figure is a sketch of the nozzle. Based on a rectangular-shaped nozzle (1.6 by 4 mm) these measurements showed that only 78 percent of the total flow cross section is illuminated, and only 31 percent was found to be within ±10 percent of constant value. Thus, the effective flow area of the instrument is not equal to the nozzle cross-sectional area. As large particles produce higher voltage pulses, it is possible for them to go through a region of lower intensity and still produce a voltage pulse greater than 0.07 volt. As an example, a 2-micrometer-diameter particle passing through the region of maximum intensity would produce a 0.28-volt pulse. It would produce a pulse greater than 0.07 volt if it passed through any point where the relative intensity was 0.25 or greater. From figure 20 this region falls within $-0.53 < x < +0.53$ millimeter, which gives a relative effective flow area of 0.66 (1.06/1.6). The relative effective flow area was calculated in the same manner for other particle diameters and is shown in figure 21. It is assumed that the calibration curve in figure 19 is based on the illumination in the region $-0.25 < x < +0.25$ millimeter.

Effect of particle number distribution. - Because effective flow area is a function of

particle diameter and because there are many more smaller particles present in a flow than larger ones, the particle count correction factor must be weighted to include a particle number distribution. The particle number distribution is generally assumed to be of the form (see ref. 18)

$$N_T = cD^{-3} \tag{1}$$

where N_T is the total number of particles greater than diameter D, c is an experimentally determined coefficient, and D is the particle diameter. Based on this equation, the following equation was used to calculate the count correction factor:

$$CCF = \frac{N_T(D_0)}{\sum_{i=0}^{20} E(D_i)\left[N_T(D_i) - N_T(D_{i+1})\right]} \tag{2}$$

for $D_i = 0.5 \times 10^{0.05\,i}$ and $E(D_i)$ is the relative effective flow area obtained from figure 21.

The numerator is a term proportional to the total number of particles greater than D_0 entering the instrument. The denominator is a term proportional to the count displayed by the instrument. The count correction factor was found to be 2.3. The data presented in this report have included this factor.

REFERENCES

1. Perkins, Porter J.; and Reck, Gregory M.: Atmospheric Constituent Measurements Using Commercial 747 Airliners. Second Joint Conf. on Sensing of Environmental Pollutants. Instrum. Soc. Am., 1973, pp. 309-318.

2. Perkins, Porter J.; and Gustafsson, Ulf R. C.: An Automated Atmospheric Sampling System Operating on 747 Airliners. Int. Conf. on Environmental Sensing and Assessment. Vol. 2, Inst. Elec. Electron. Eng., Inc., pp. 1 26-4 to 10 26-4.

3. Holdeman, James D.; and Falconer, Phillip D.: Analysis of Atmospheric Ozone Measurements Made From a B-747 Airliner During March 1975. NASA TN D-8311, 1976.

4. Reck, Gregory M.; Briehl, Daniel; and Perkins, Porter J.: Flight Test of a Pressurization System Used to Measure Minor Atmospheric Constituents from an Aircraft. NASA TN D-7576, 1974.

5. Briehl, Daniel; et al.: Nitric Oxide, Water Vapor, and Ozone in the Atmosphere as Measured In-Situ from an Aircraft. NASA TM X-3174, 1975.

6. Briehl, D.: In-Situ Measurements of Particulate Number Density and Size Distribution from an Aircraft. 2nd Int. Conf. on the Environmental Impact of Aerospace Operations in the High Atmosphere. Am. Meteorological Soc., 1974, pp. 16-18.

7. Grobecker, A. J.; Coroniti, S. C.; and Cannon, R. H., Jr.: Report of Findings: The Effects of Stratospheric Pollution by Aircraft. DOT-TST-75-50, 1974.

8. Bowman, Lloyd D.; and Horak, Richard F.: A Continuous Ultraviolet Absorption Ozone Photometer. Anal. Instrum., vol. 10, 1972, pp. 103-108.

9. Saltzman, Bernard E.; and Gilbert, Nathan: Iodometric Microdetermination of Organic Oxidants and Ozone. Anal. Chem., vol. 31, no. 11, Nov. 1959, pp. 1914-1920.

10. Link, W. T.; et al.: A Fluorescent Source NDIR Carbon Monoxide Analyzer. AIAA Paper 71-1047, 1971.

11. Lin, B. Y. H.; Berglum, R. N.; and Agarwal, J. K.: Experimental Studies of Optical Particle Counters. Publ. 209, Univ. of Minnesota, Particle Technol. Lab., 1973.

12. Hilsenrath, E.: High Altitude Aircraft Water Vapor Measurements. AIAA Paper 73-511, June 1973.

13. Goodman, P.; and Chleck, D.: Calibration of the Panametrics Aluminum Oxide Hygrometer. Anal. Instru., vol. 7, 1969, p. 233.

14. Hasegawa, Saburo; et al.: A Laboratory Study of Some Performance Characteristics of An Aluminum Oxide Humidity Sensor. NBS TN-824, Nat. Bur. Stand., 1974.

15. Vanderhoff, J. A.: Time Response Characteristics of An Aluminum Oxide Sensor. J. Geophys. Res., vol. 79, no. 15, May 1974, pp. 2207-2214.

16. Bader, M.; and Wagoner, C. B.: NASA Program of Airborne Optical Observations. Opt., vol. 9, Feb. 1970, pp. 265-270.

17. Seiler, W.; and Warneck, P.: Decrease of the Carbon Monoxide Mixing Ratio at the Tropopause. J. Geophys. Res., vol. 77, no. 18, June 1972, pp. 3204-3213.

18. Williamson, Samuel J.: Fundamentals of Air Pollution. Addison-Wesley Publishing Co., 1973.

TABLE I. - ARCTIC EXPERIMENT FLIGHTS

(a) Phase I

Flight	Date	Route (b)	Type of flight	Figure
[a]1	3/25/75	SFO-SFO	------	-----
[a]2	3/27/75	SFO-SFO	------	-----
3	3/31/75	SFO-ANC	Ferry	12(a)
[a]4	4/5/75	ANC-ANC	Marine survey	-----
5	4/6/75	ANC-ANC	↓	11(a)
6	4/7/75	ANC-ANC	↓	11(b)
7	4/8/75	ANC-ANC	↓	11(c)
8	4/9/75	ANC-SFO	Ferry	12(b)
9	4/12/75	SFO-FAI	Ferry	12(c)
10	4/13/75	FAI-FAI	Ice camp	10(a)
11	4/16/75	FAI-THU	Polar	9(a)
12	4/17/75	THU-THU	Polar	9(b)
13	4/19/75	THU-FAI	Polar	9(c)
14	4/21/75	FAI-FAI	Ice camp	10(b)
15	4/22/75	FAI-FAI	↓	10(c)
16	4/24/75	FAI-FAI	↓	10(d)
17	4/26/75	FAI-FAI	↓	10(e)
18	4/27/75	FAI-SFO	Ferry	12(d)

(b) Phase II

[a]1	8/12/75	SFO-SFO	------	-----
[a]2	8/13/75	SFO-SFO	------	-----
3	8/15/75	SFO-FAI	Ferry	16(a)
4	8/18/75	FAI-FAI	Ice camp	13(a)
[a]5	8/19/75	FAI-FAI	Marine survey	-----
6	8/22/75	FAI-FAI	Ice camp	13(b)
[a]7	8/23/75	FAI-FAI	Marine survey	-----
[a]8	8/24/75	FAI-FAI	Marine survey	-----
9	8/27/75	FAI-FAI	Ice camp	13(c)
[a]10	8/28/75	FAI-FAI	Marine survey	-----
11	8/29/75	FAI-SFO	Ferry	16(b)

(c) Phase III

[a]1	10/4/75	SFO-SFO	-----	-----
2	10/8/75	SFO-FAI	Ferry	18(a)
3	10/10/75	FAI-FAI	Ice camp	17(a)
[a]4	10/11/75	FAI-FAI	Marine survey	-----
[a]5	10/14/75	FAI-FAI	Marine survey	-----
6	10/15/75	FAI-FAI	Ice camp	17(b)
[a]7	10/18/75	FAI-FAI	Marine survey	-----
8	10/20/75	FAI-FAI	Ice camp	17(c)
9	10/22/75	FAI-FAI	Ice camp	17(d)
[a]10	10/23/75	FAI-FAI	Marine survey	-----
[a]11	10/25/75	FAI-FAI	Marine survey	-----
12	10/26/75	FAI-FAI	Ice camp	17(e)
[a]13	10/27/75	FAI-FAI	Marine survey	-----
14	10/29/75	FAI-SFO	Ferry	18(b)

[a]Data from these flights are not presented in this report.

[b]Cities of origin and destination: SFO, San Francisco (including Moffet Field), Calif.; ANC, Anchorage, Alaska; FAI, Fairbanks, Alaska; THU, Thule, Greenland.

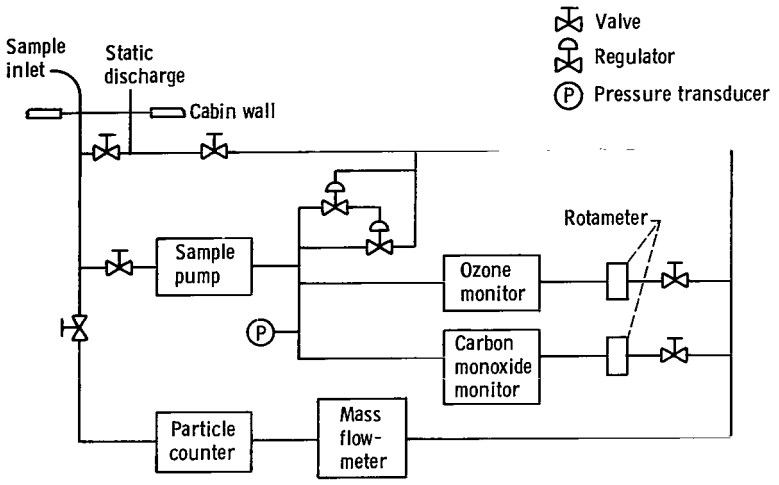

Figure 1. - Schematic of sampling system used in all phases.

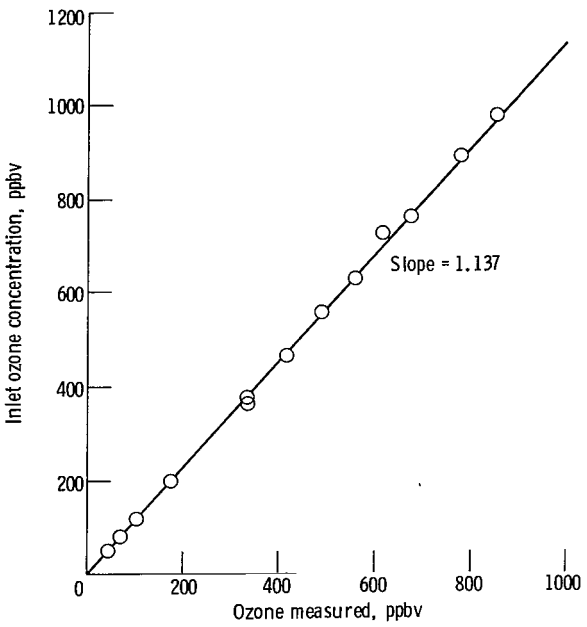

Figure 2. - Effect of sampling system on ozone concentration.

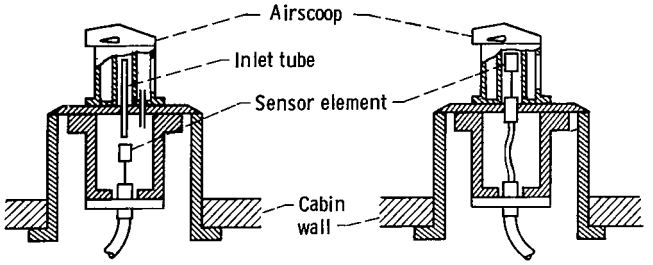

(a) Aluminum oxide hygrometer, chamber mount.

(b) Aluminum oxide hygrometer, scoop mount.

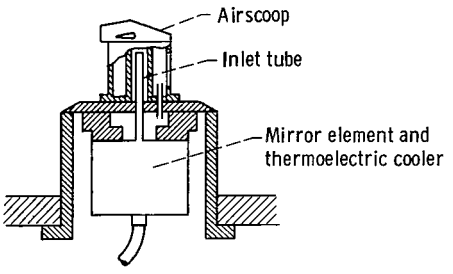

(c) Cooled-mirror hygrometer.

Figure 3. - Hygrometer probe sketches.

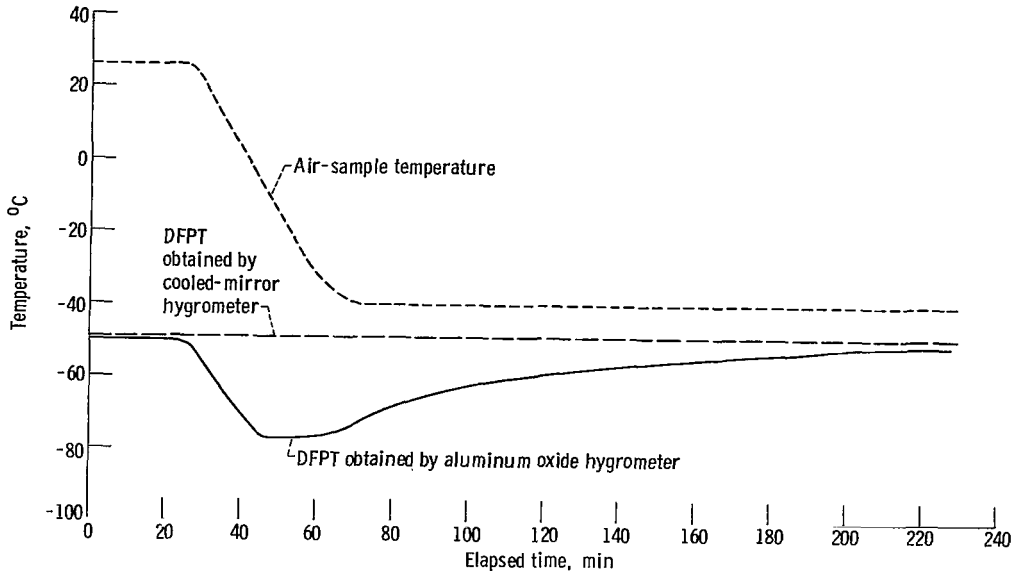

Figure 4. - Response of an aluminum oxide hygrometer to change in ambient temperature with no change in dew-frost point temperature (DFPT).

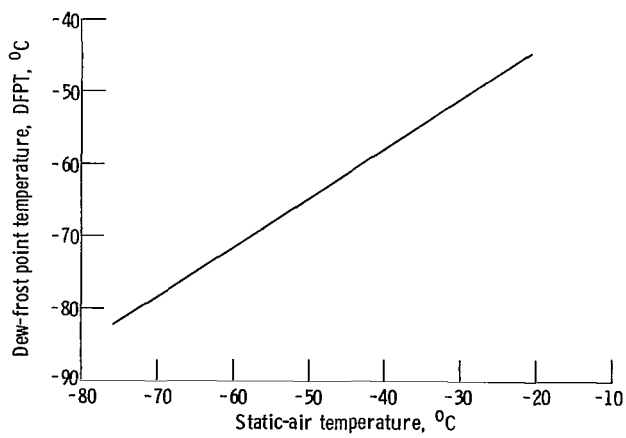

Figure 5. - Minimum or lowest dew-frost point temperature capability of cooled-mirror hygrometer at flight Mach 0.82.

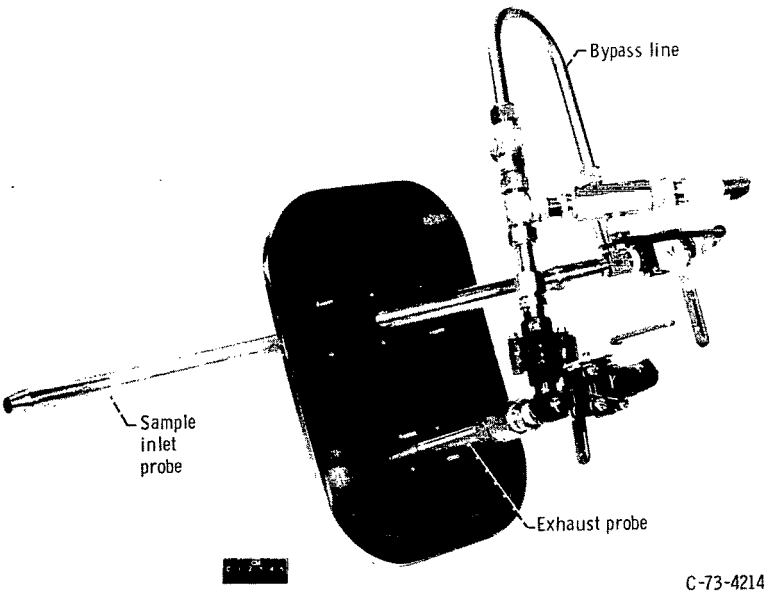

(a) Sample probe assembly.

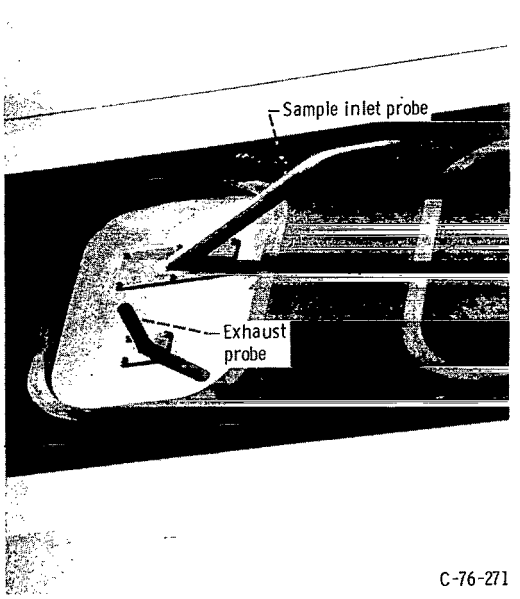

(b) Sample probe installation.

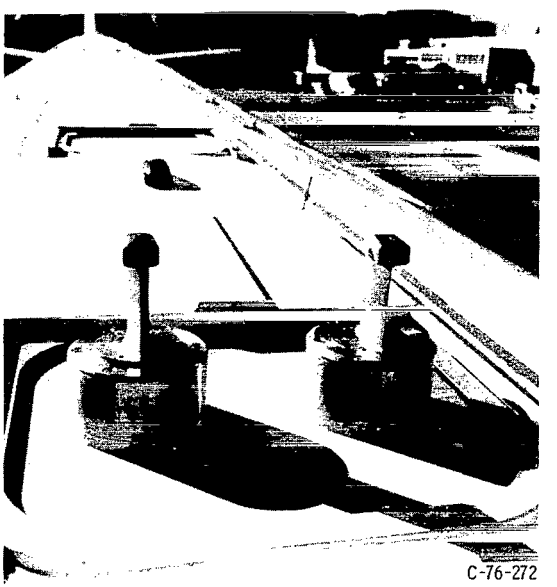

(c) Hygrometer probe installation.

Figure 6. - Sample probe assemblies and installation aboard CV-990 aircraft.

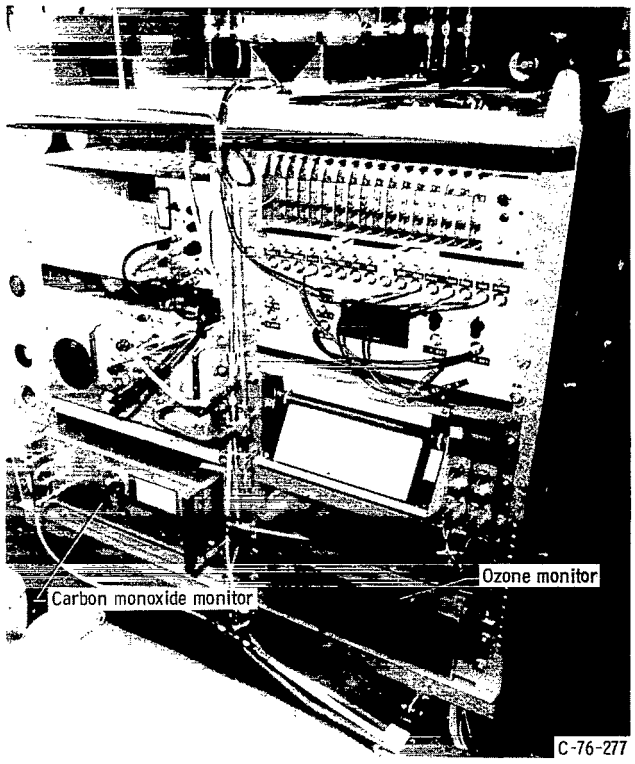

(a) Port equipment rack.

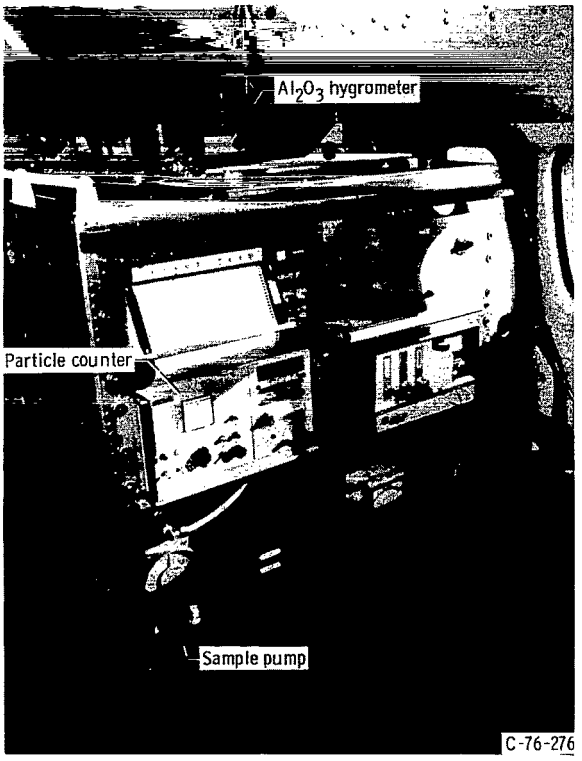

(b) Starboard equipment rack.

Figure 7. - Sampling equipment installation in CV-990 equipment racks.

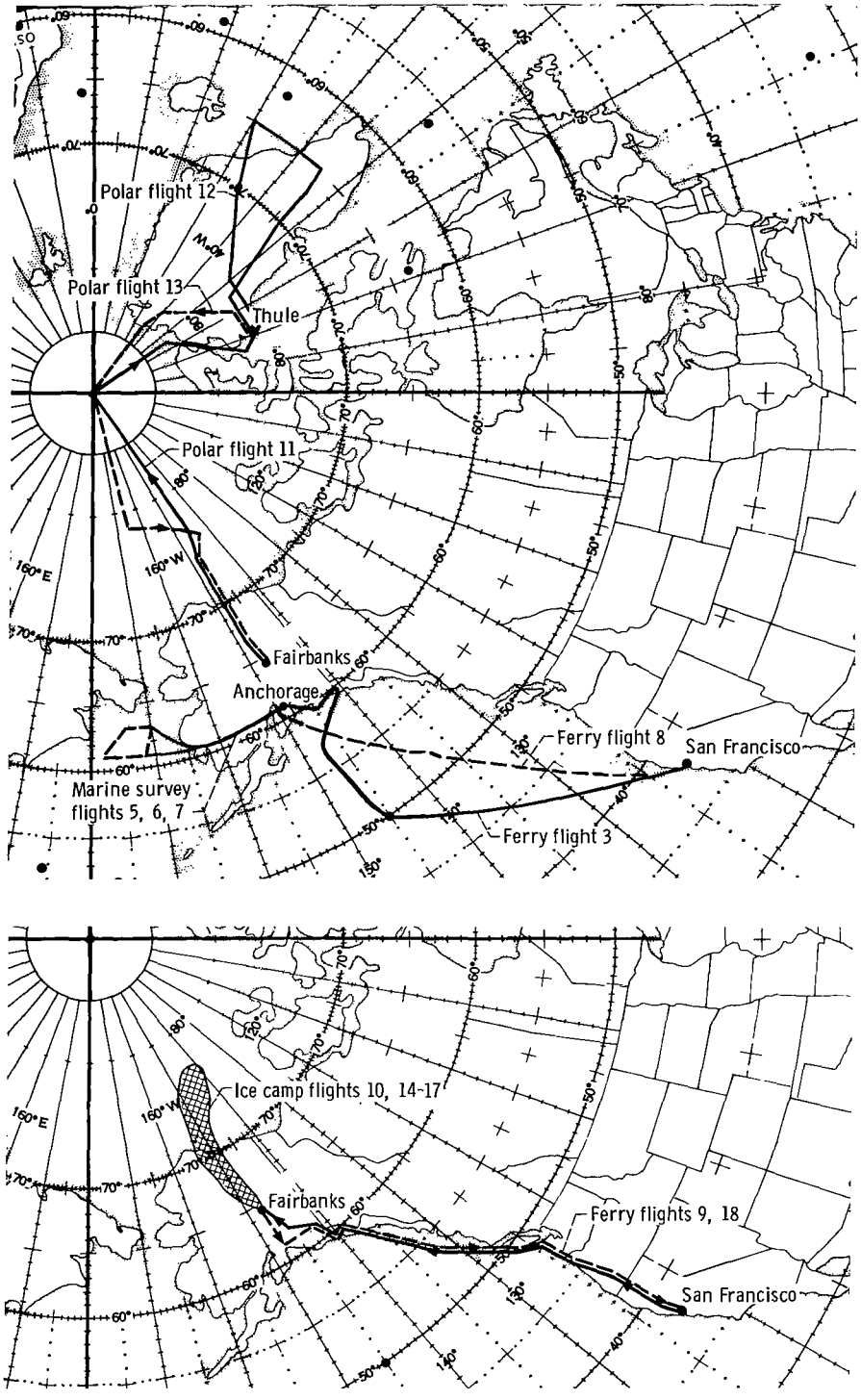

(a) Phase I, April 1975.

Figure 8. - Arctic flight routes.

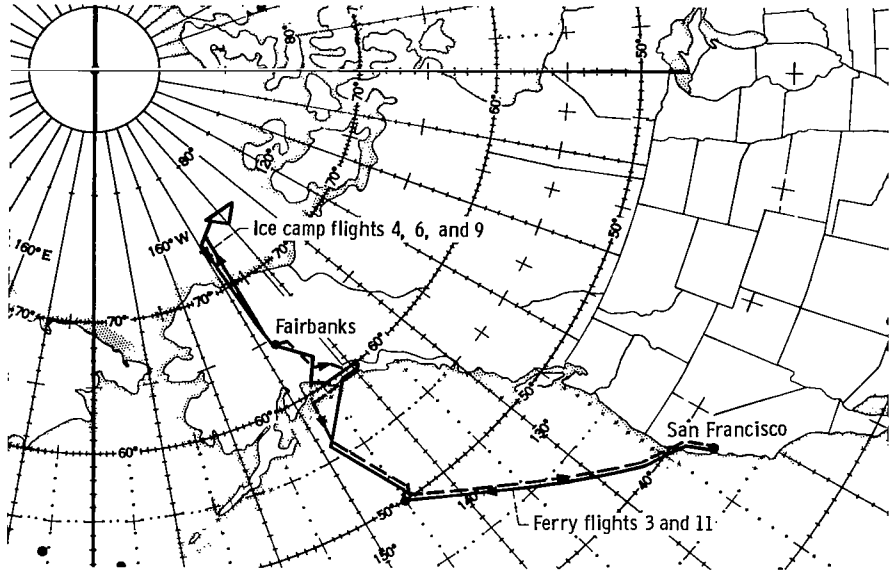

(b) Phase II flight routes, August 1975.

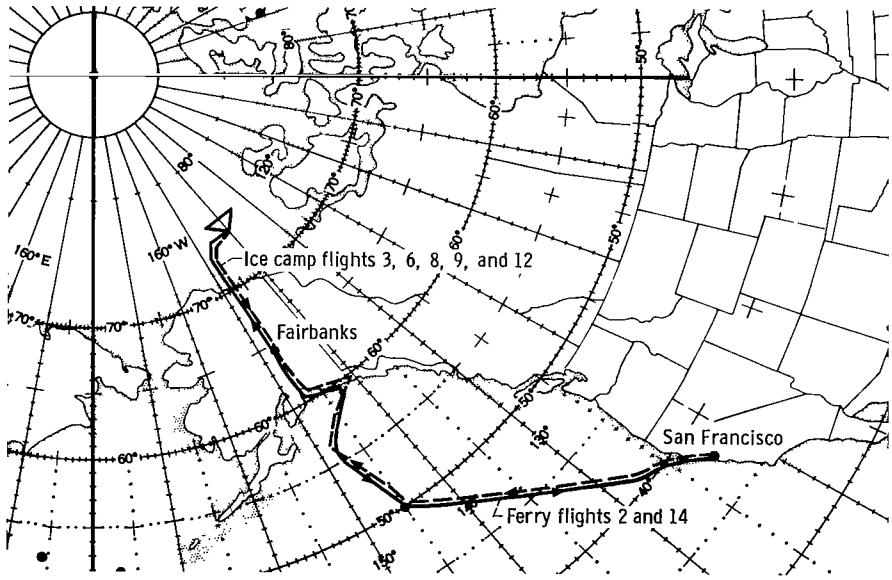

(c) Phase III flight routes, October 1975.

Figure 8. - Concluded.

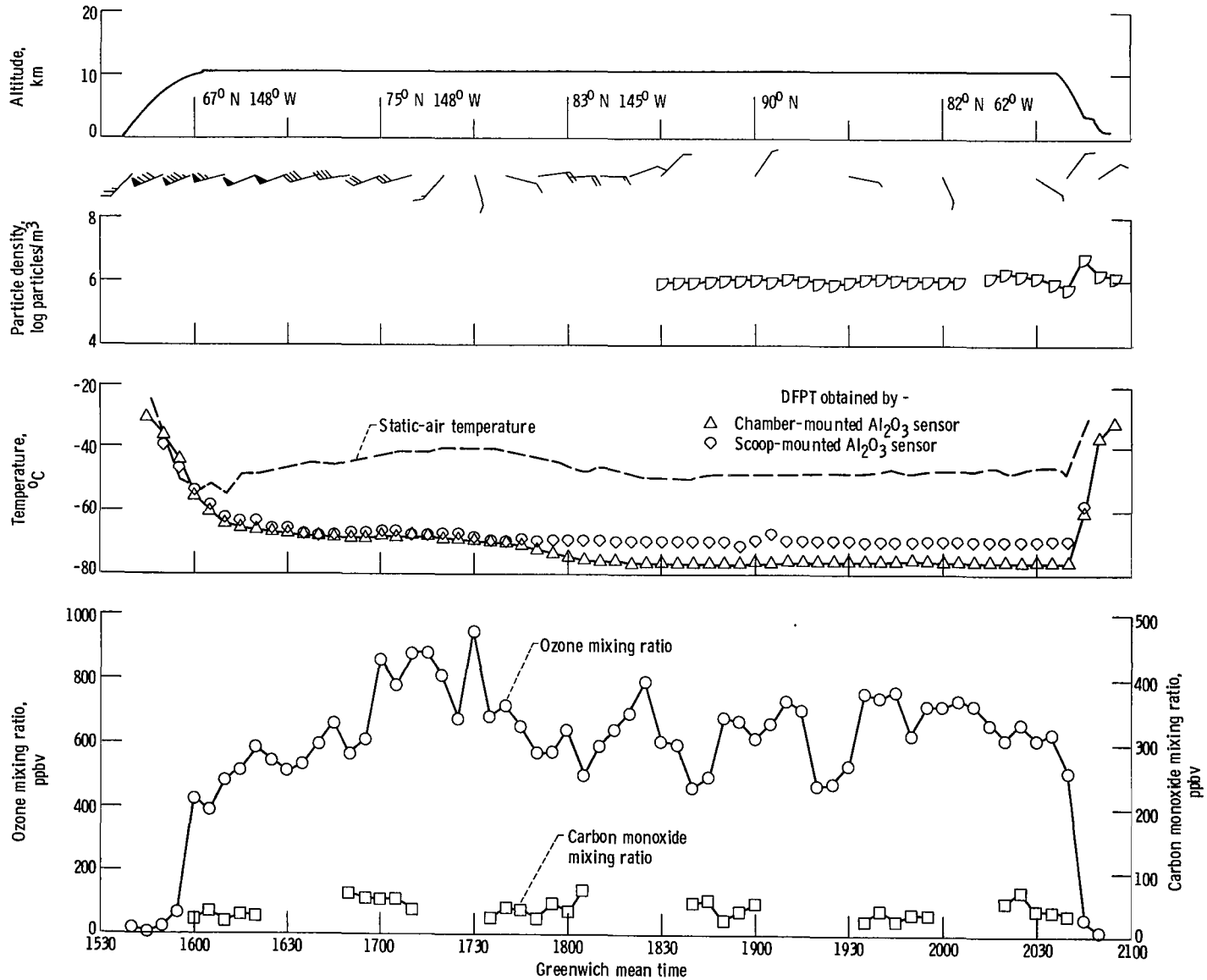

(a) Flight 11: April 16, 1975, Fairbanks to Thule.

Figure 9. - Polar flight data obtained during phase I.

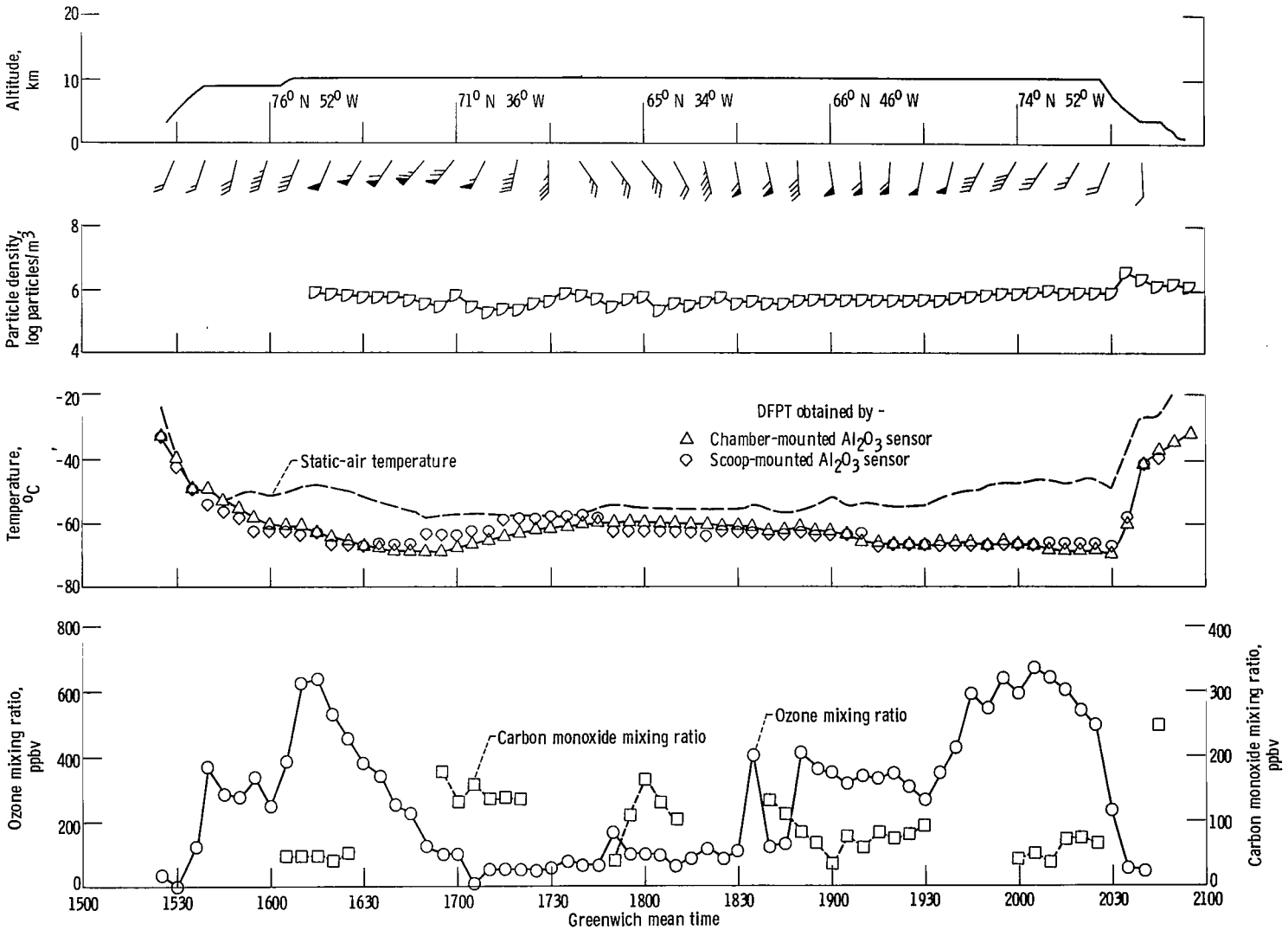

(b) Flight 12: April 17, 1975, Thule to Thule.

Figure 9. - Continued.

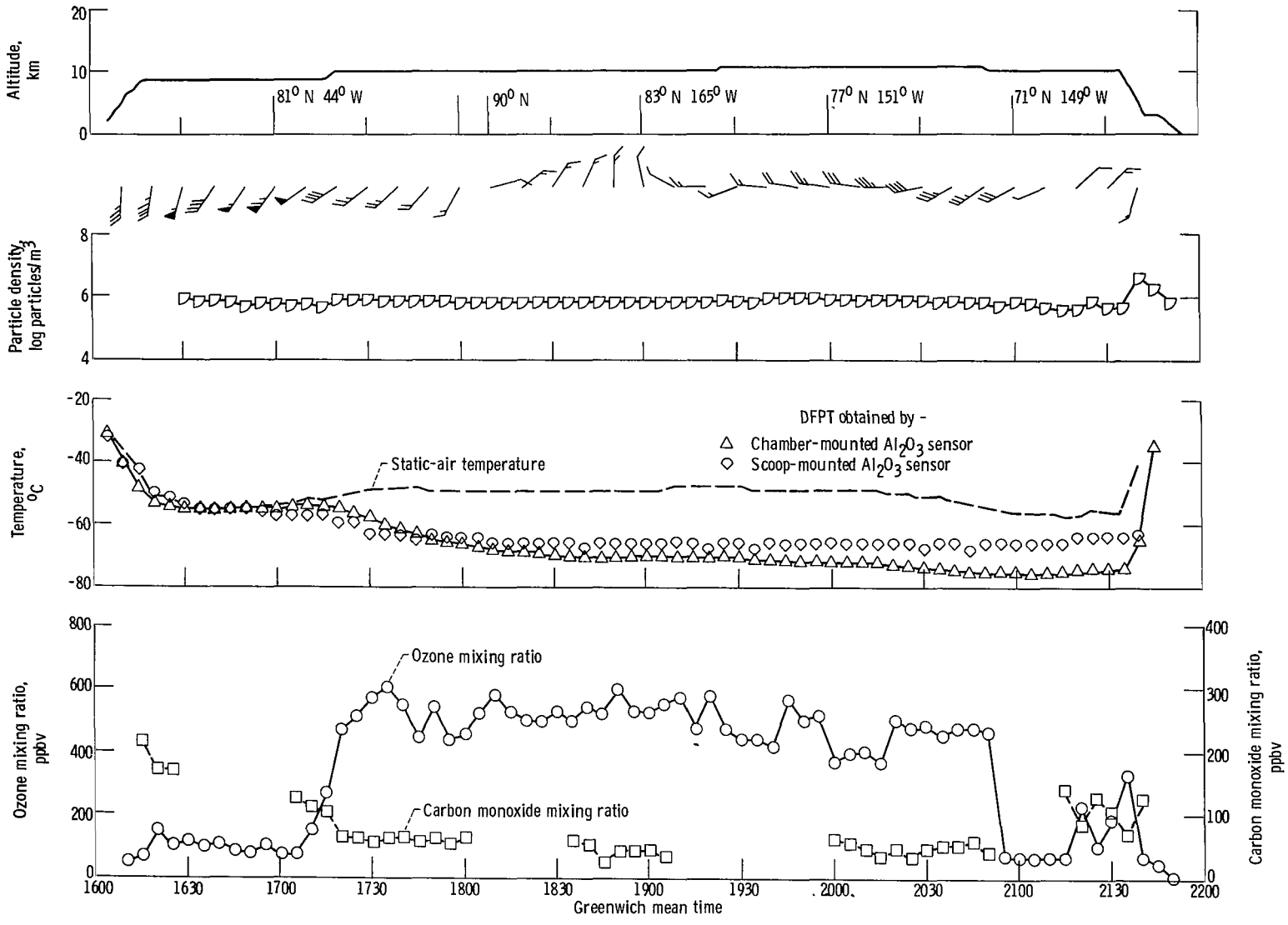

(c) Flight 13, April 19, 1975, Thule to Fairbanks.

Figure 9. - Concluded.

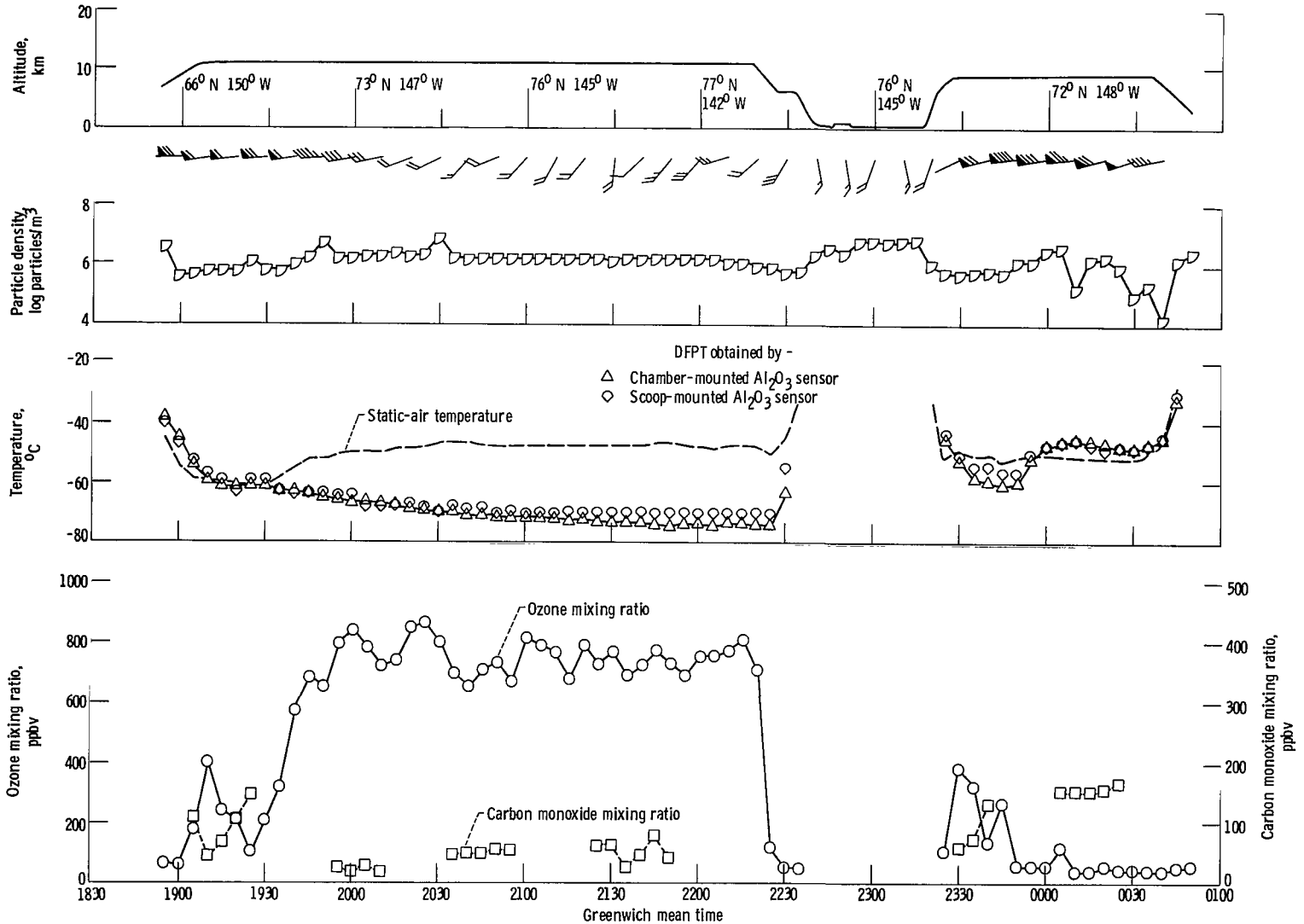

(a) Flight 10: April 13, 1975, Fairbanks to Fairbanks.

Figure 10. - Ice camp flight data obtained during phase I.

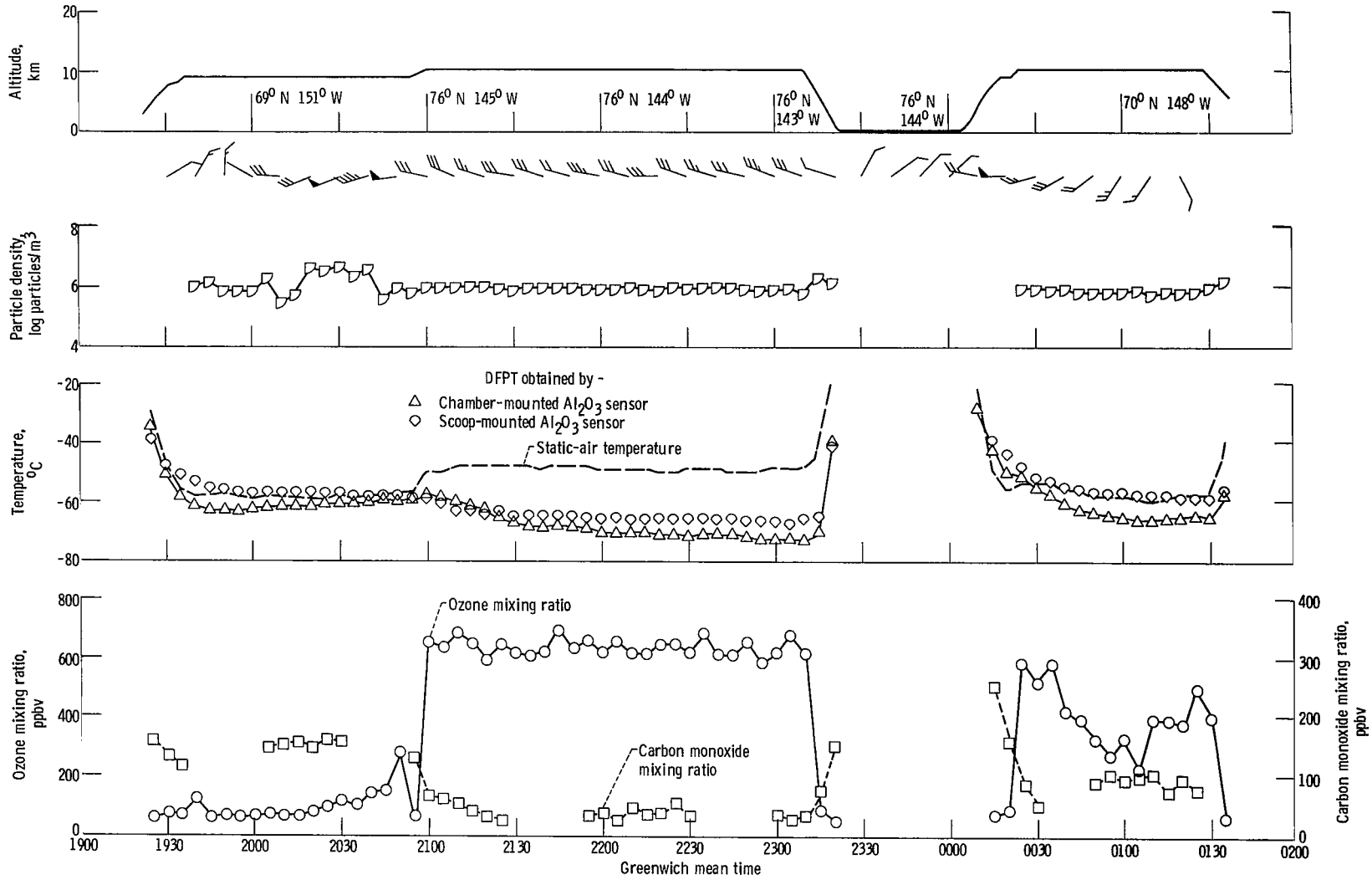

(b) Flight 14: April 21, 1975, Fairbanks to Fairbanks.

Figure 10. - Continued.

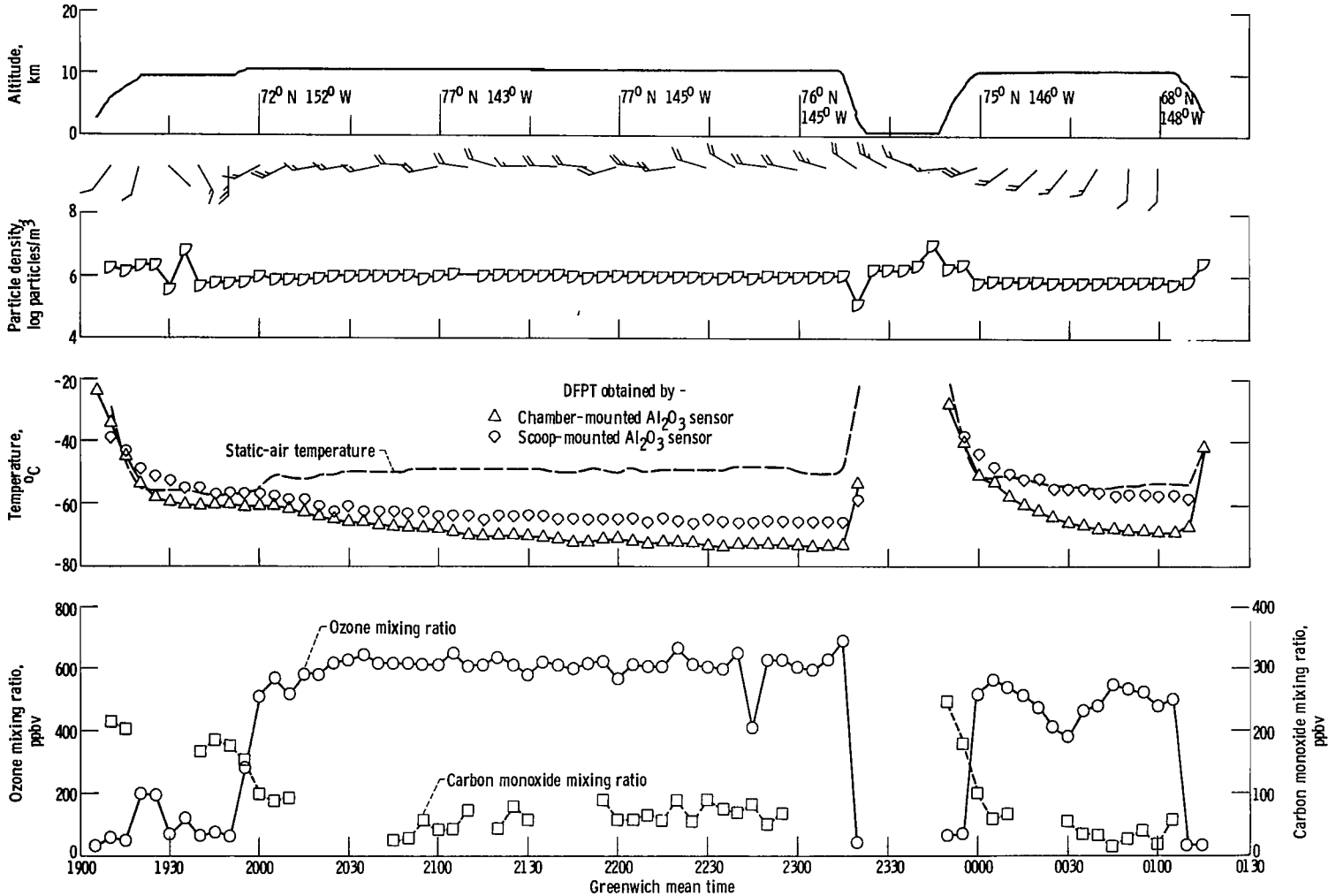

(c) Flight 15: April 22, 1975, Fairbanks to Fairbanks.

Figure 10. - Continued.

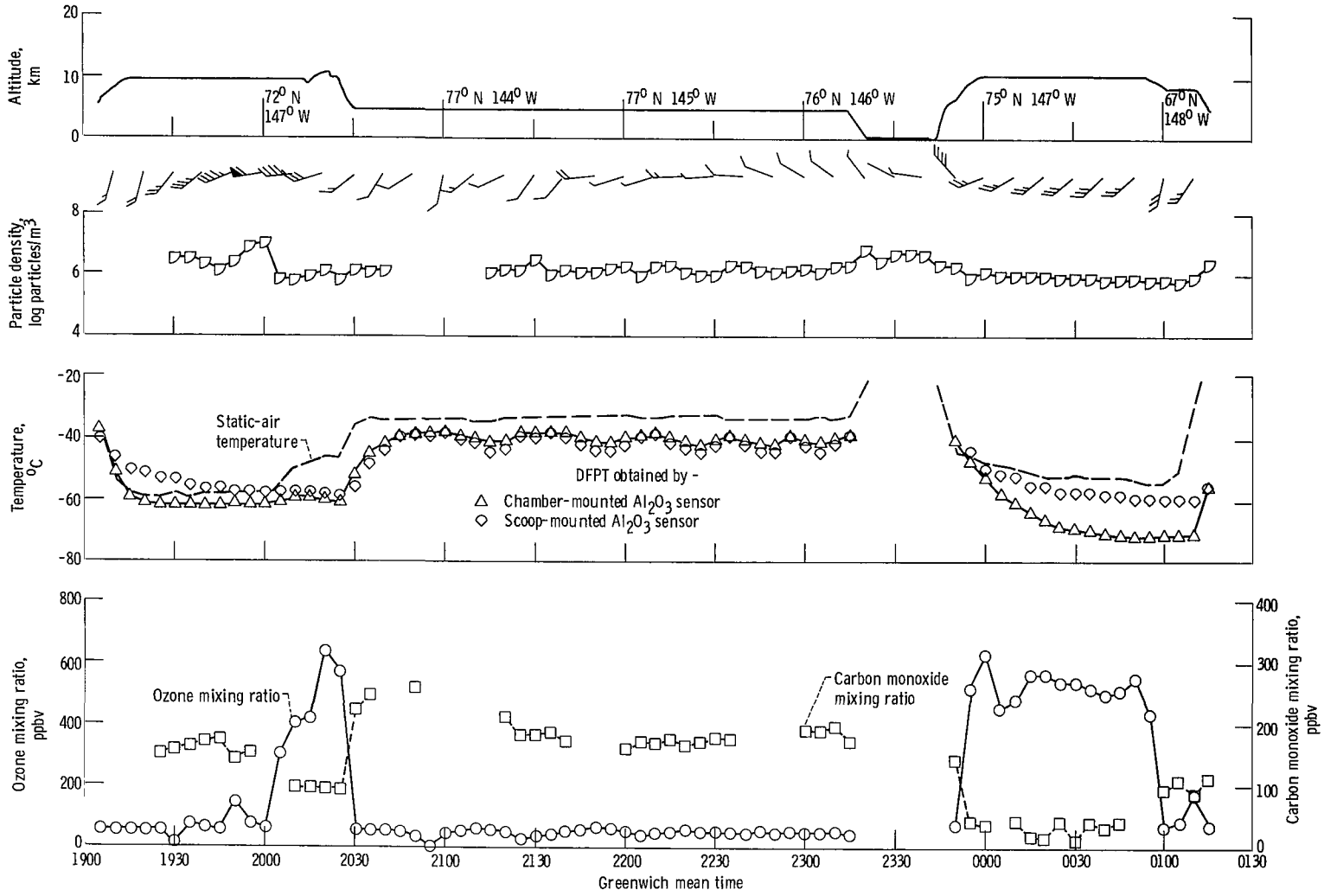

(d) Flight 16: April 24, 1975, Fairbanks to Fairbanks.

Figure 10. - Continued.

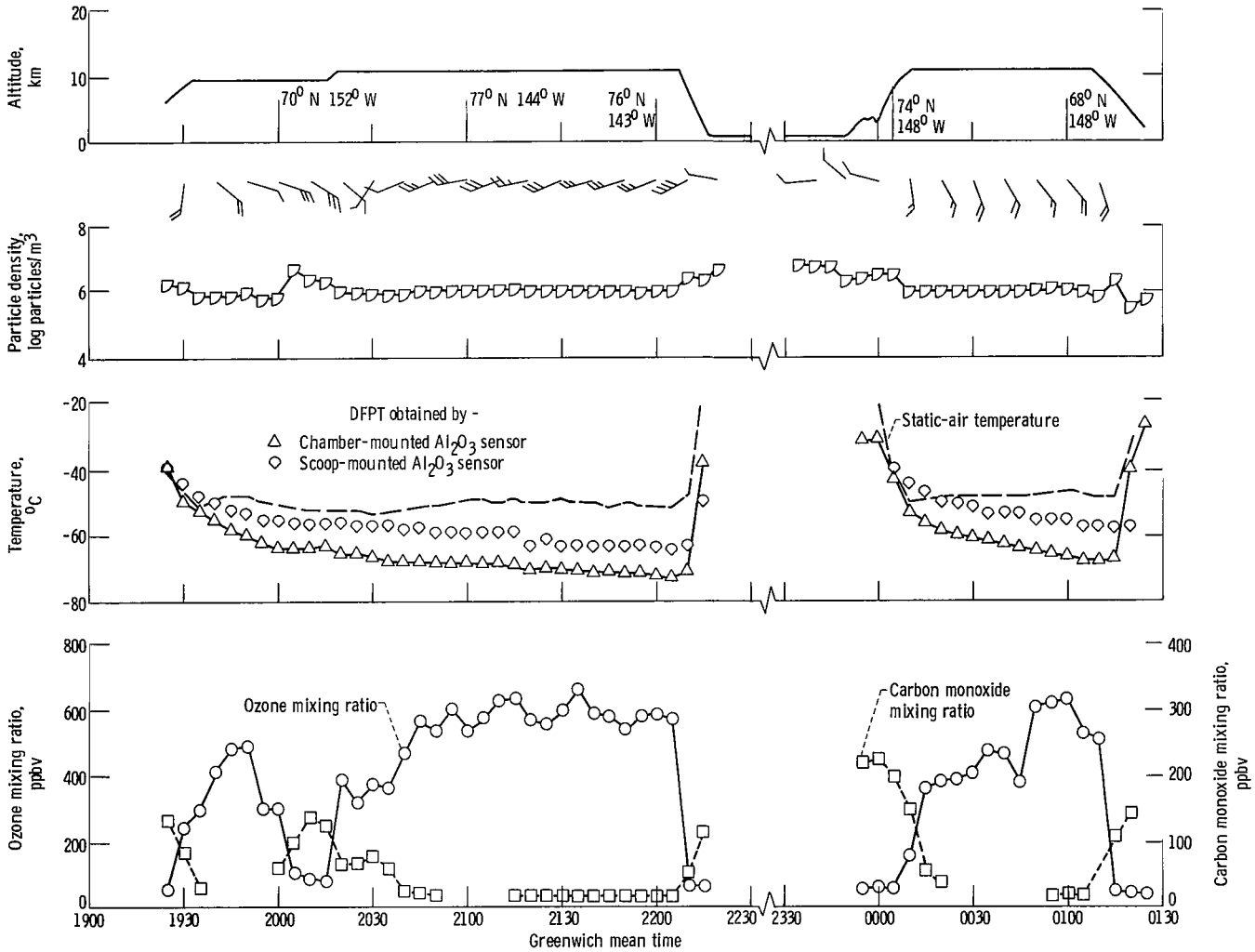

(e) Flight 17: April 26, 1975, Fairbanks to Fairbanks.

Figure 10. - Concluded.

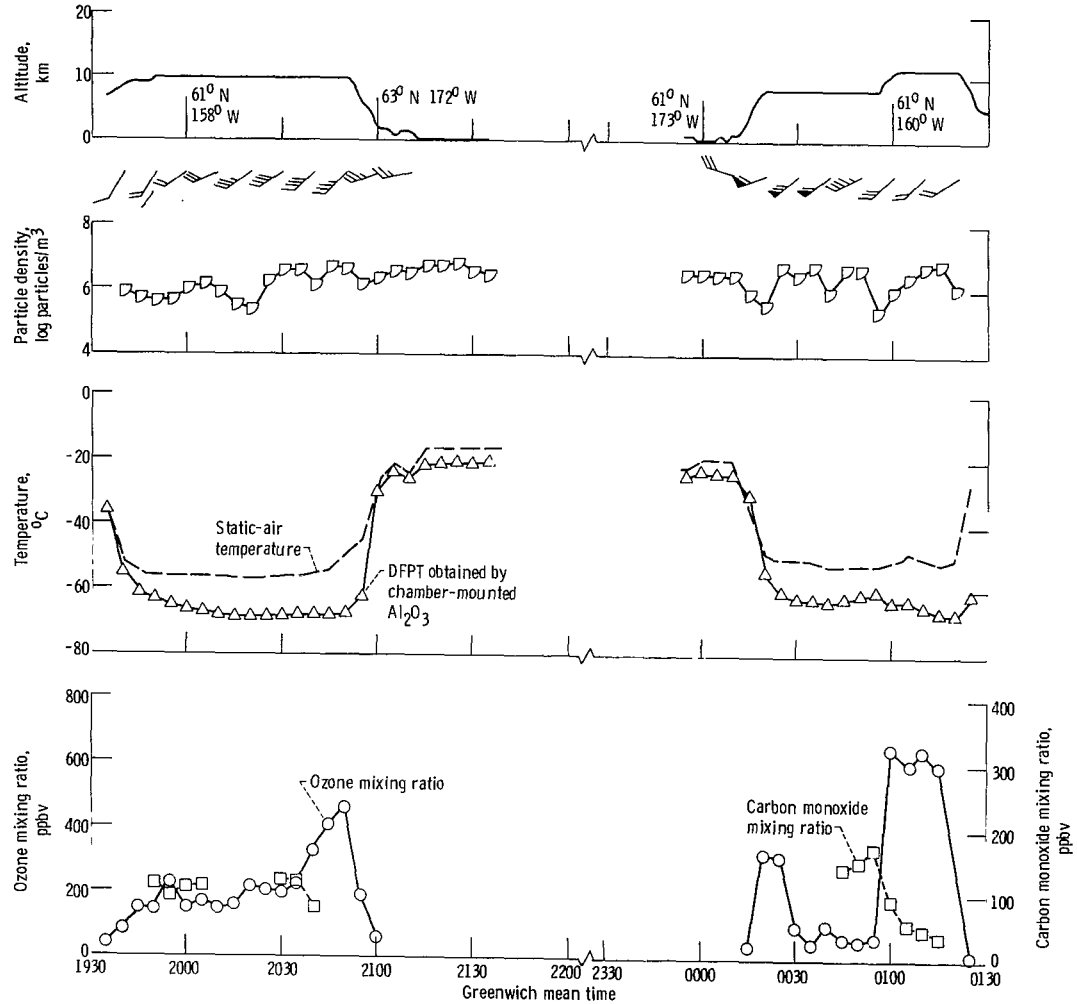

(a) Flight 5; April 6, 1975, Anchorage to Anchorage.

Figure 11. - Marine survey flight data during phase I.

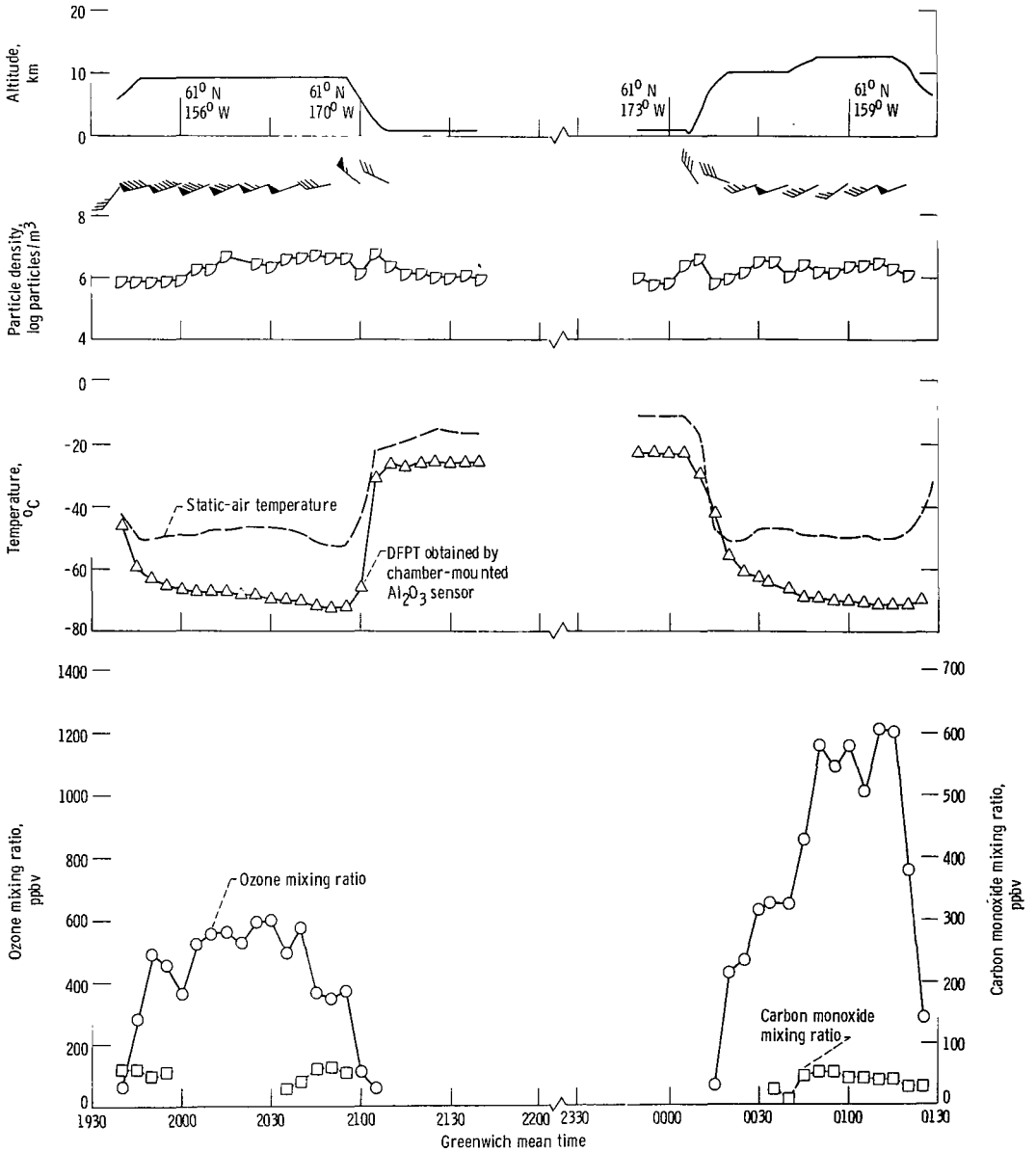

(b) Flight 6: April 7, 1975, Anchorage to Anchorage.

Figure 11. - Continued.

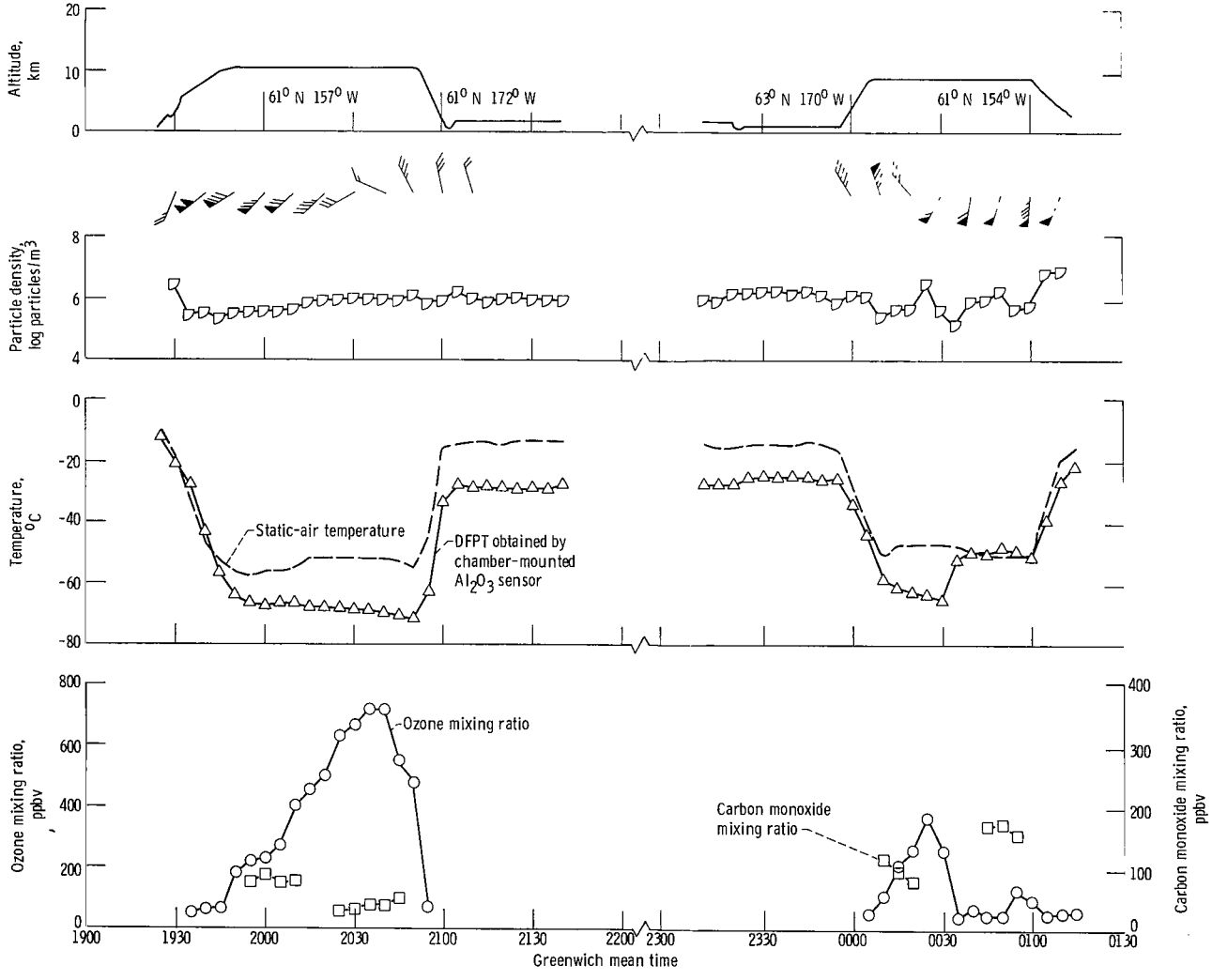

(c) Flight 7: April 8, 1975, Anchorage to Anchorage.

Figure 11. - Concluded.

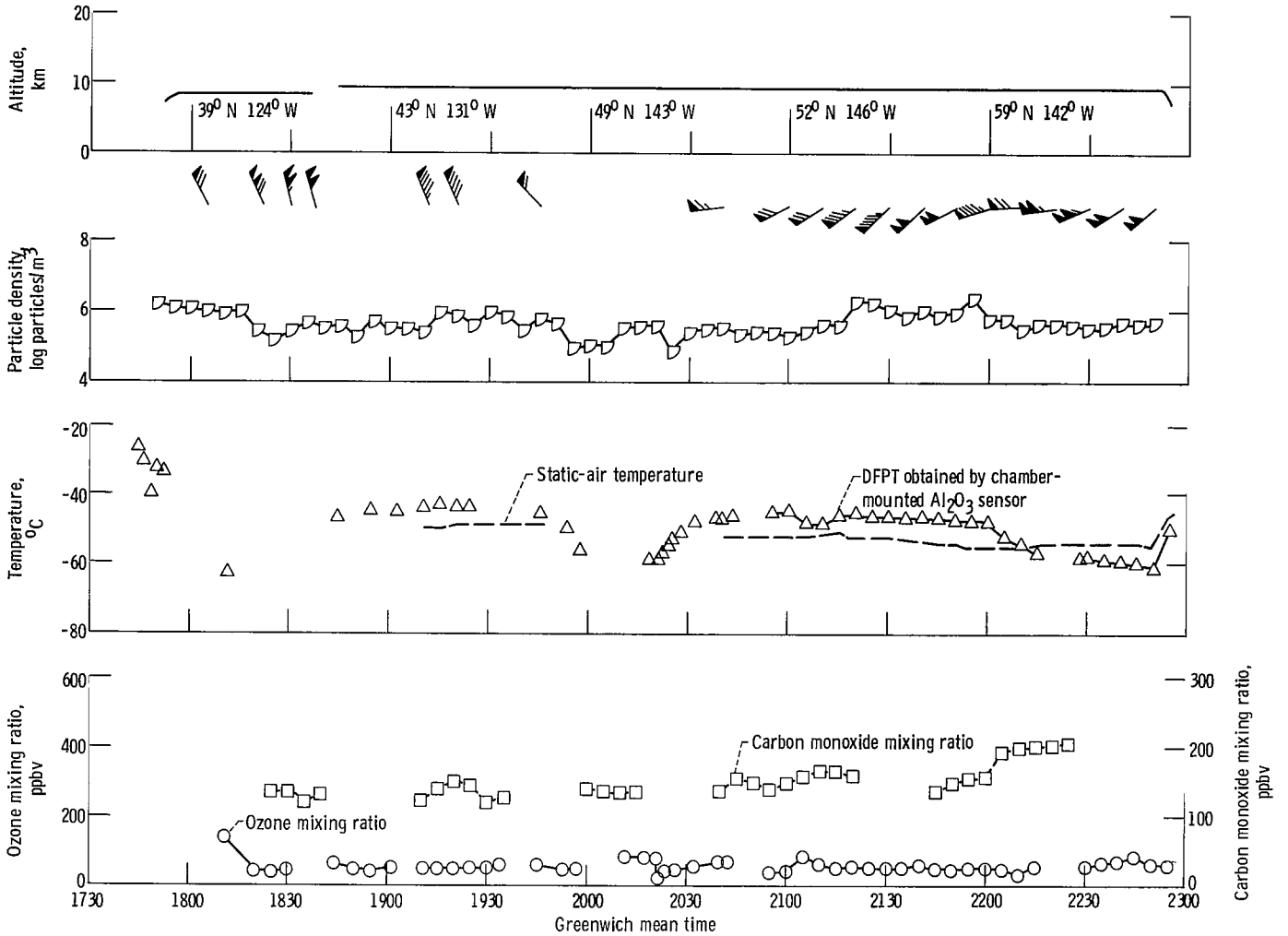

(a) Flight 3; March 31, 1975, Moffett Field to Anchorage.

Figure 12. - Ferry flight data obtained during phase I.

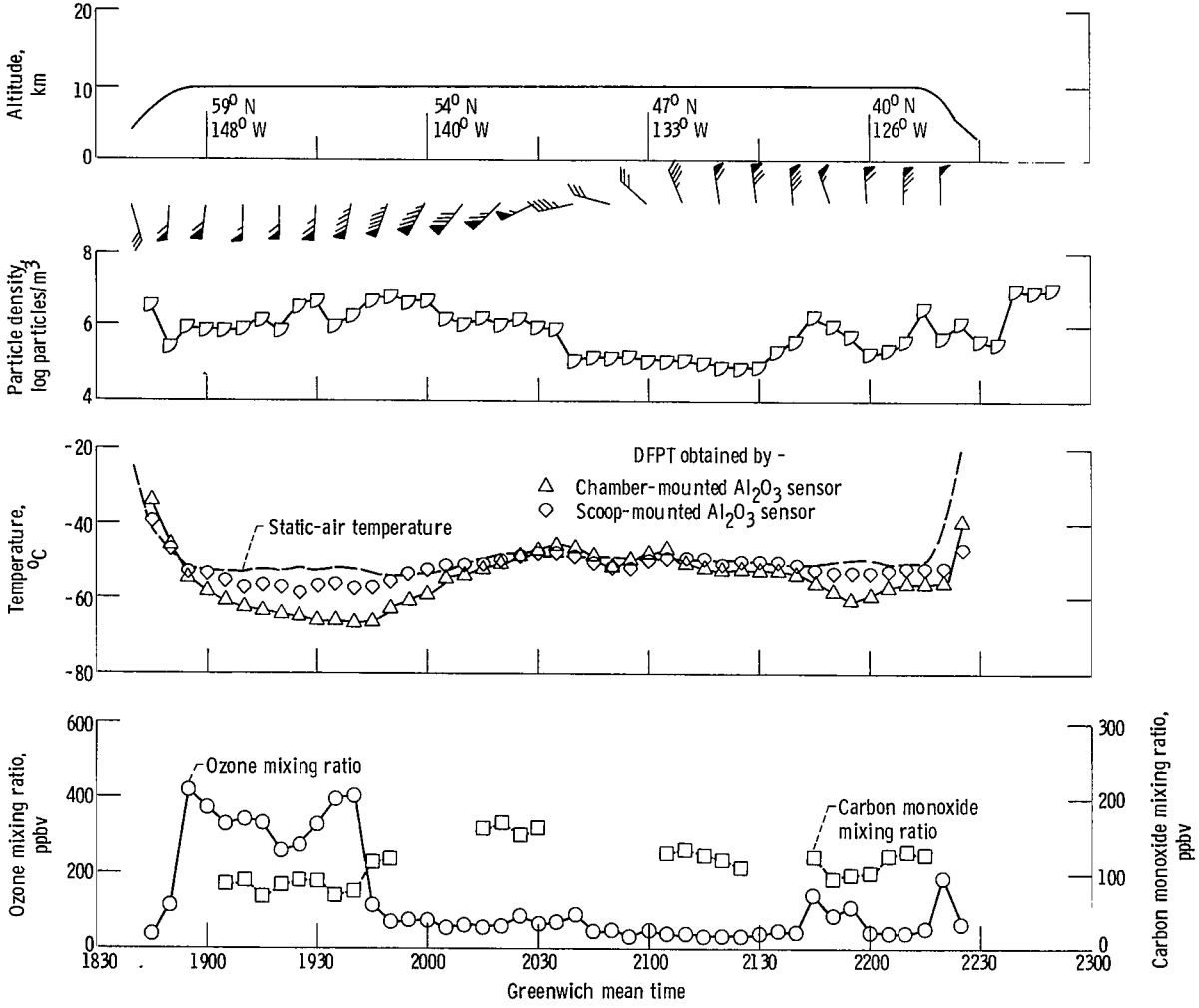

(b) Flight 8: April 9, 1975, Anchorage to Moffett Field.

Figure 12. - Continued.

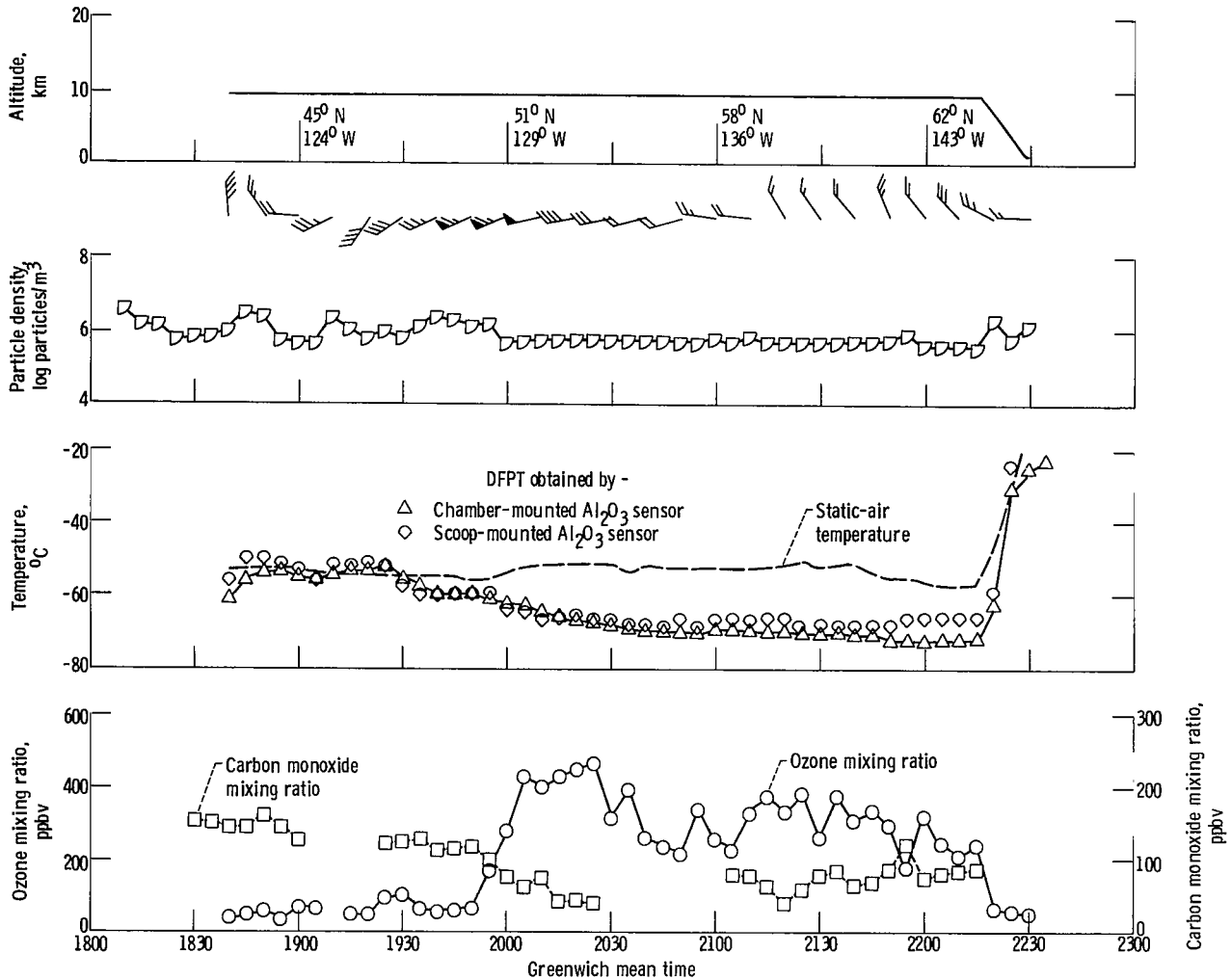

(c) Flight 9: April 12, 1975, Moffett Field to Fairbanks.

Figure 12. - Continued.

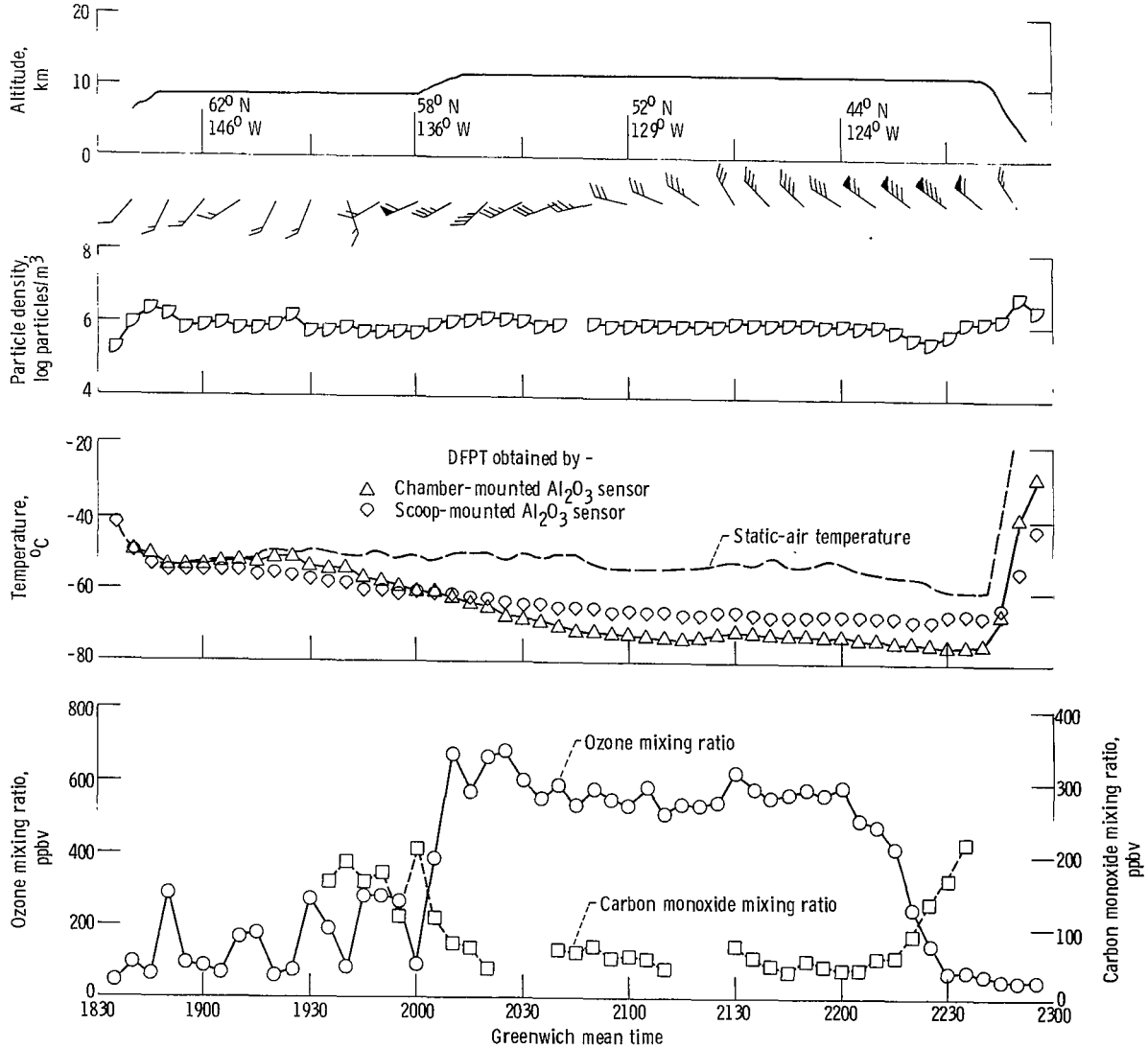

(d) Flight 18: April 27, 1975, Fairbanks to Moffett Field.

Figure 12. - Concluded.

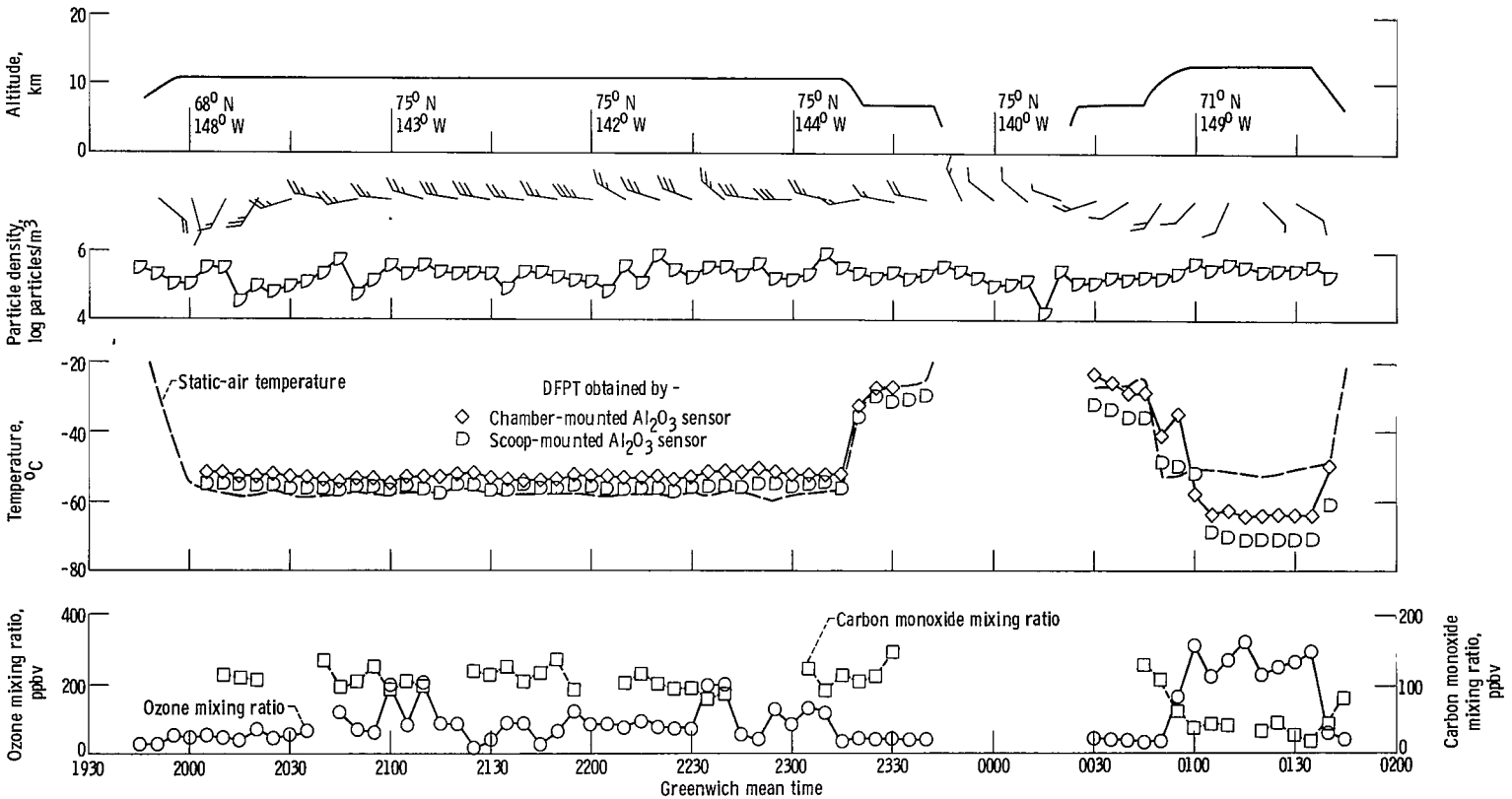

(a) Flight 4: August 18, 1975, Fairbanks to Fairbanks.

Figure 13. - Ice camp flight data obtained during phase II.

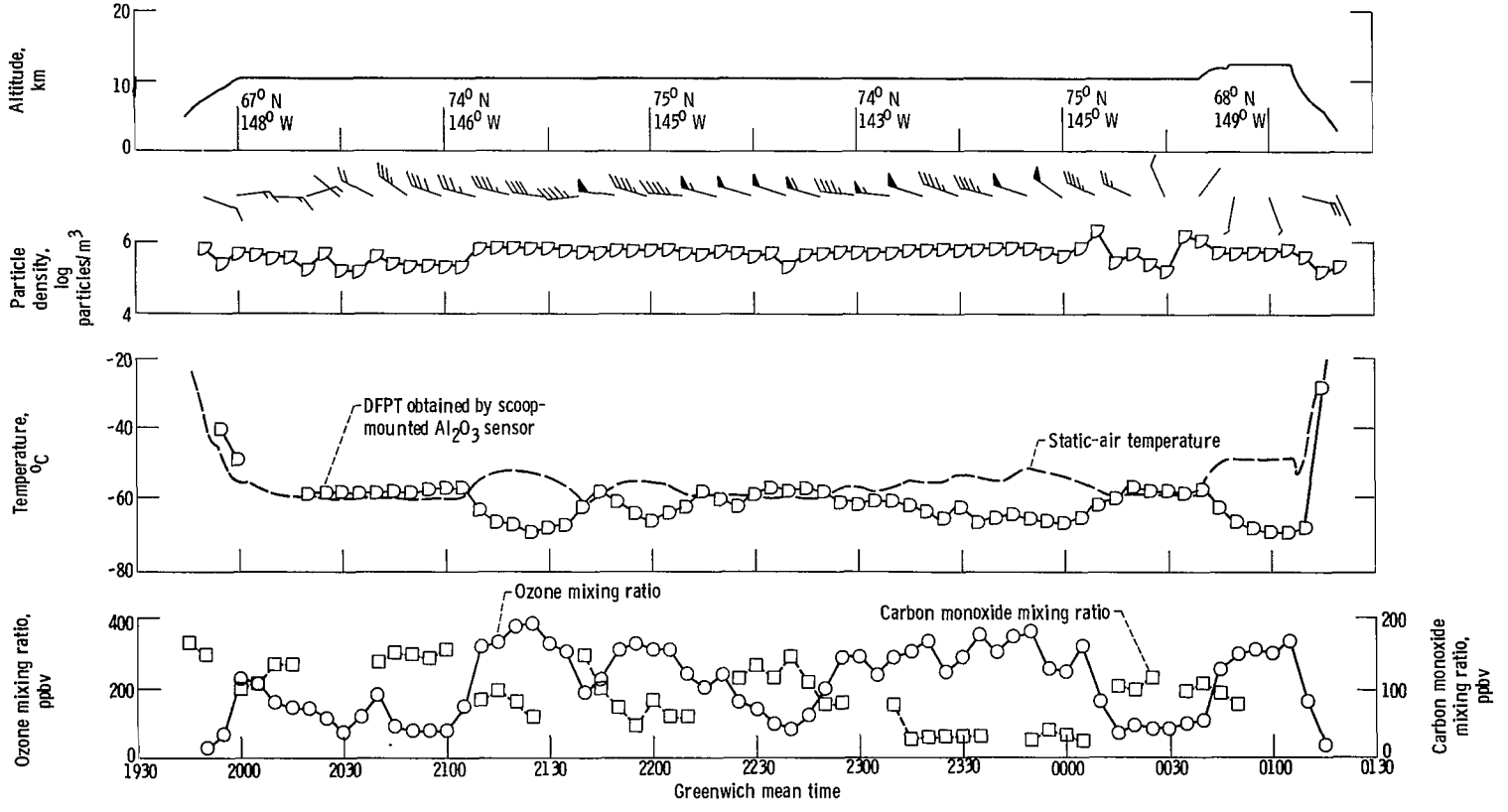

(b) Flight 6: August 22, 1975, Fairbanks to Fairbanks.

Figure 13. - Continued.

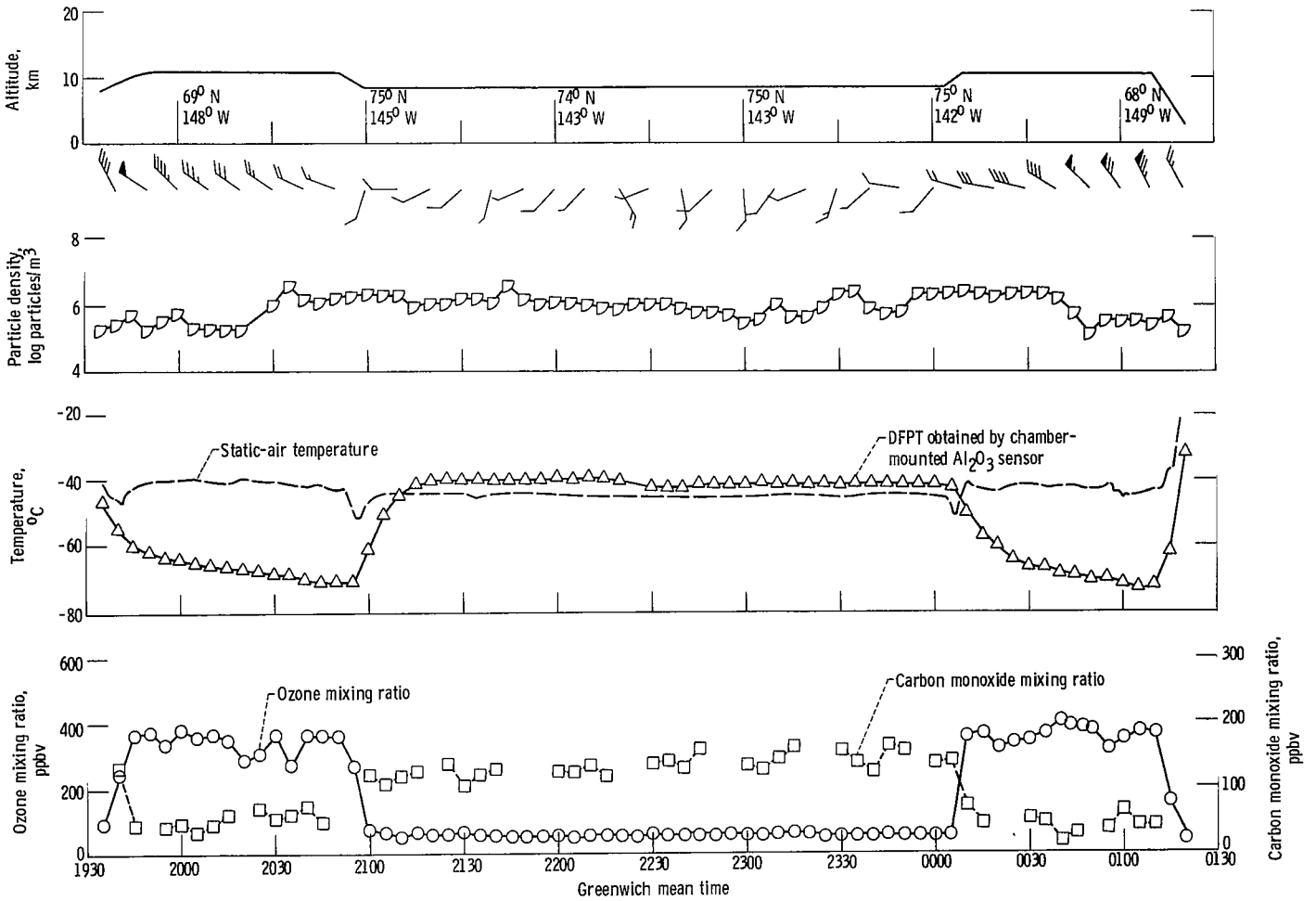

(c) Flight 9: August 27, 1975, Fairbanks to Fairbanks.

Figure 13. - Concluded.

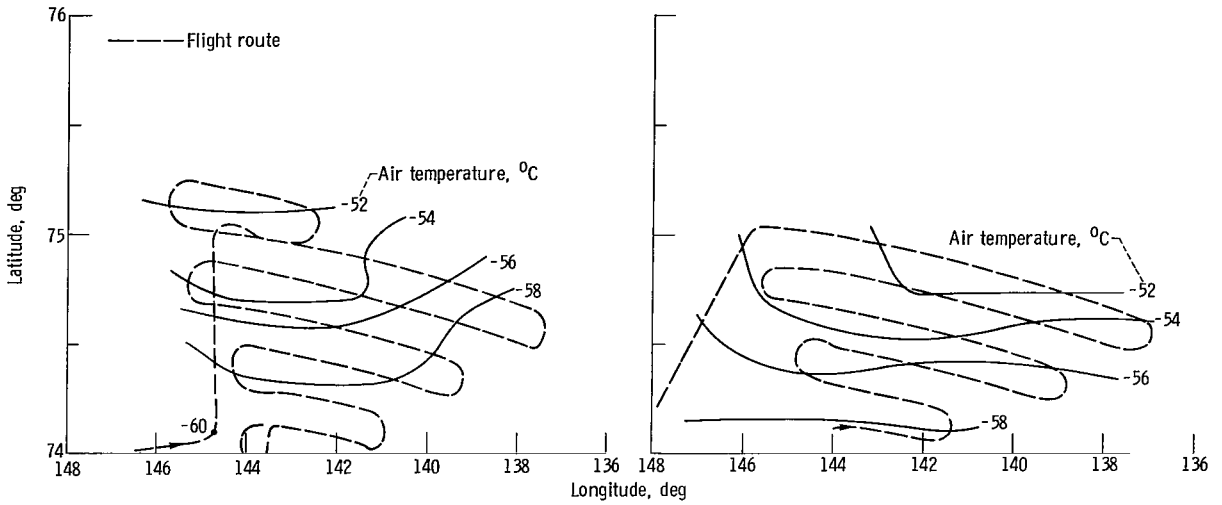

(a) Initial runs; time, 2100 to 2240 GMT.

(b) Final runs; time, 2240 to 0010 GMT.

Figure 14. - Isotherms over ice camps. Phase II, flight 6; altitude, 10.7 kiometers.

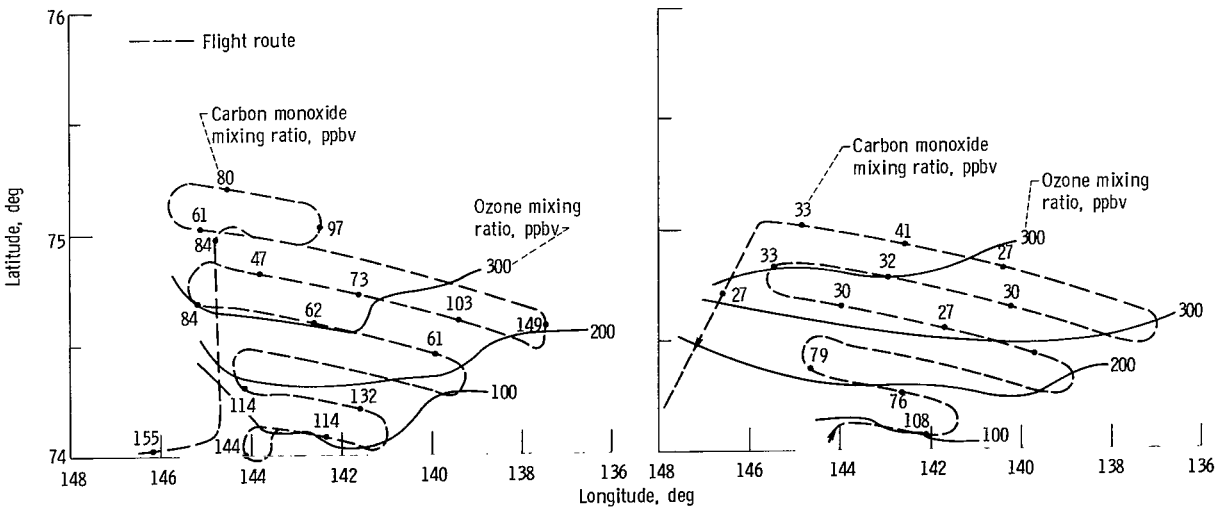

(a) Initial runs; time, 2100 to 2240 GMT.

(b) Final runs; time, 2240 to 0010 GMT.

Figure 15. - Ozone isopleths and carbon monoxide data obtained during pattern runs over ice camps. Phase II, flight 6; altitude, 10.7 kilometers.

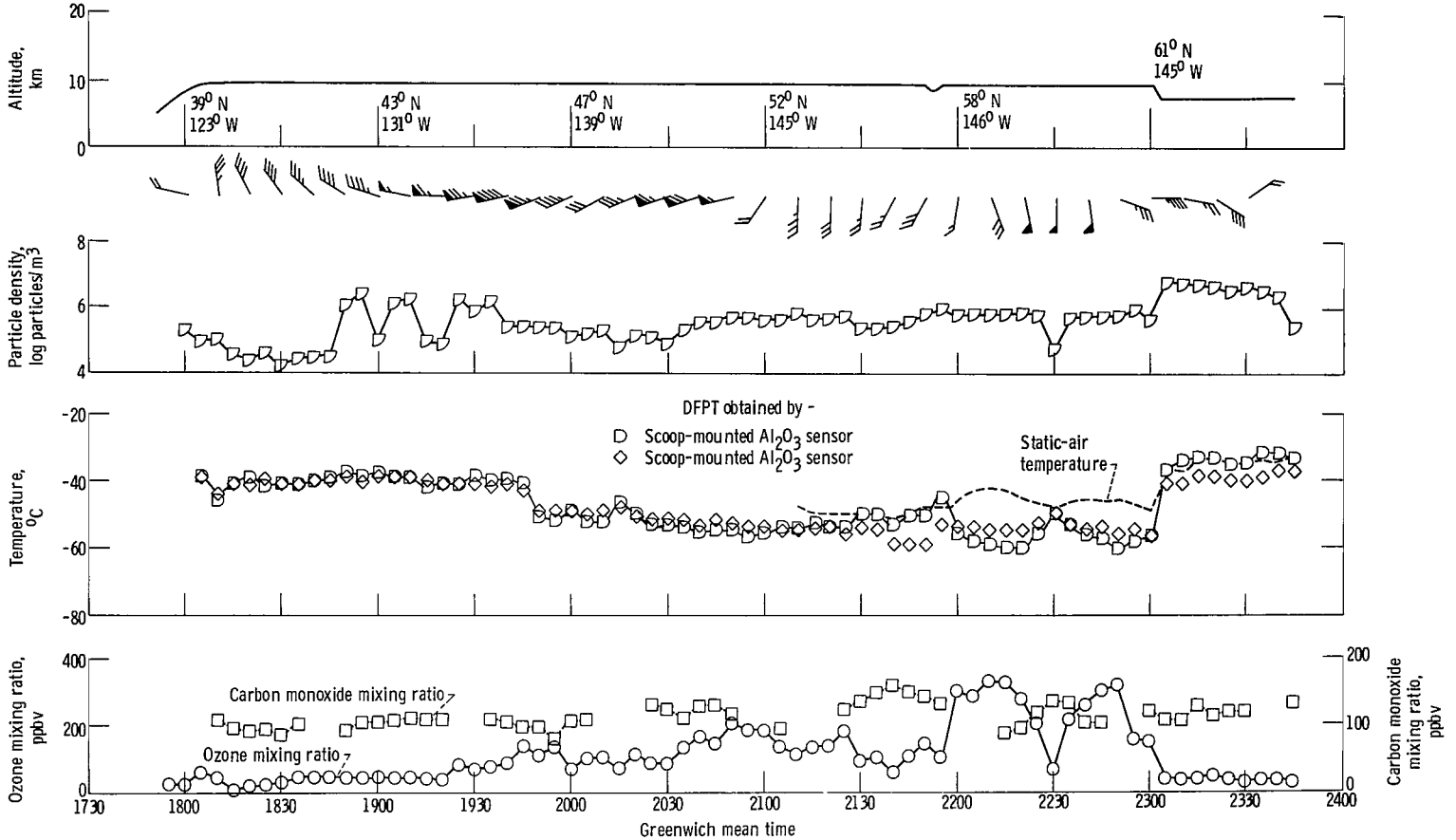

(a) Flight 3: August 15, 1975, Moffett Field to Fairbanks.

Figure 16. - Ferry flight data obtained during phase II.

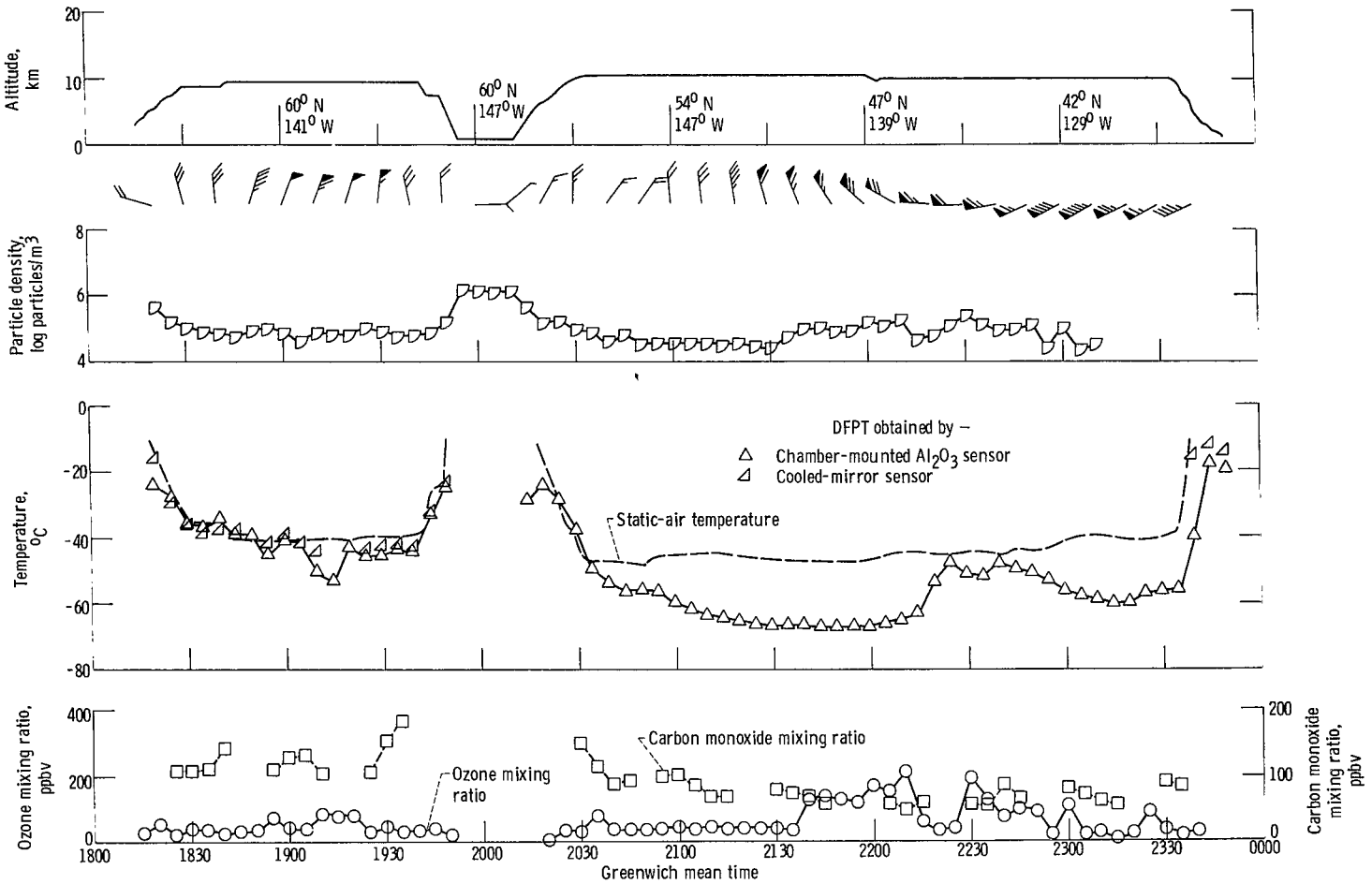

(b) Flight 11: August 29, 1975, Fairbanks to Moffett Field.

Figure 16. - Concluded.

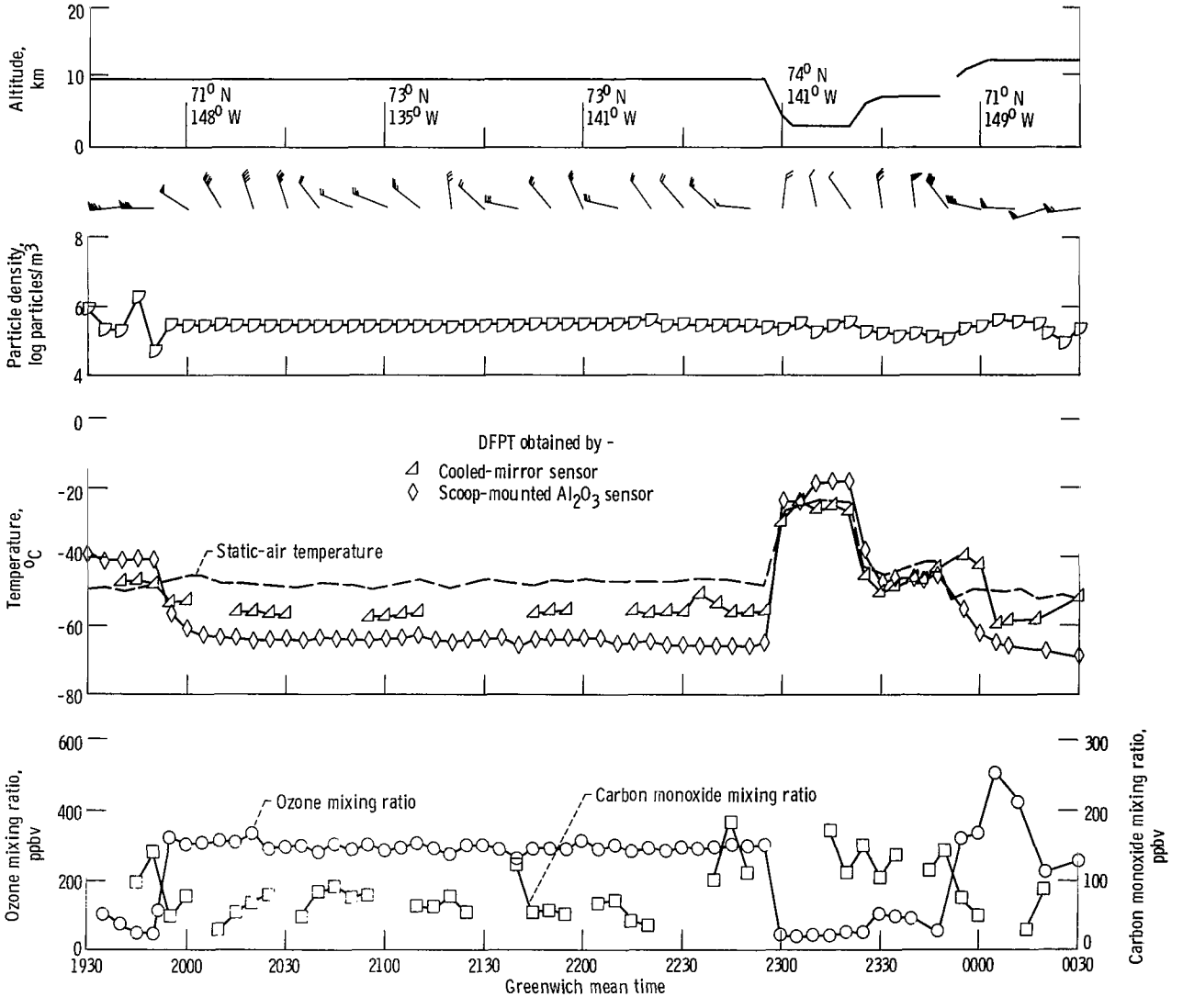

(a) Flight 3: October 10, 1975, Fairbanks to Fairbanks.

Figure 17. - Ice camp flight data obtained during phase III.

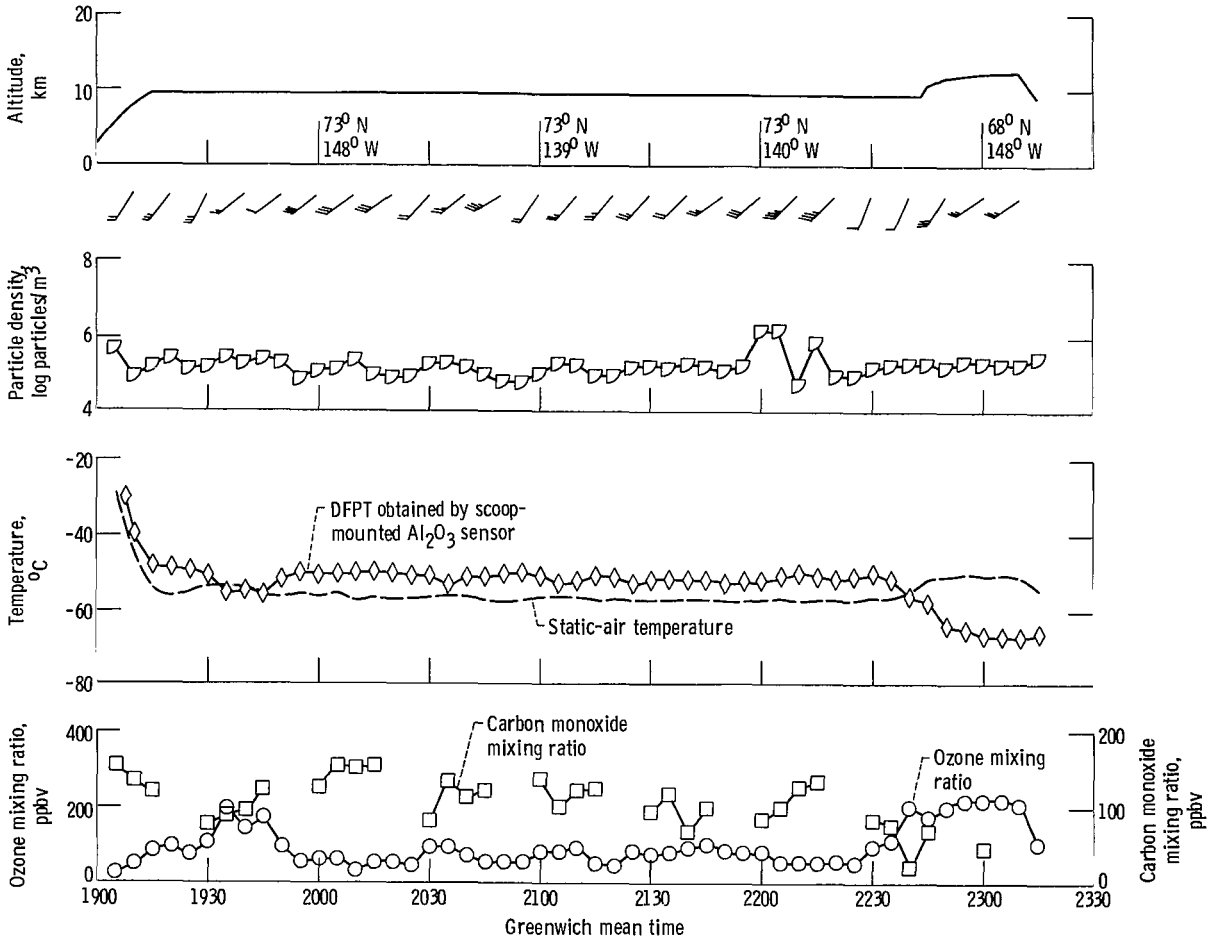

(b) Flight 6: October 15, 1975, Fairbanks to Fairbanks.

Figure 17. - Continued.

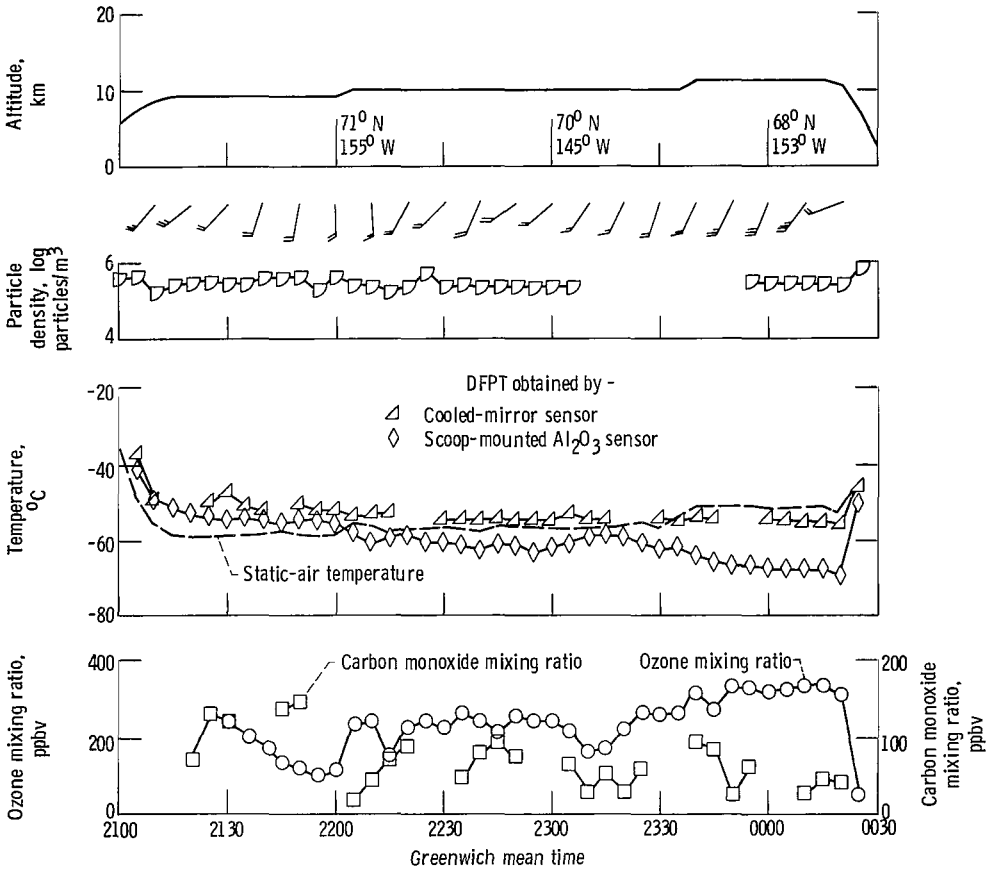

(c) Flight 8: October 20, 1975, Fairbanks to Fairbanks.

Figure 17. - Continued.

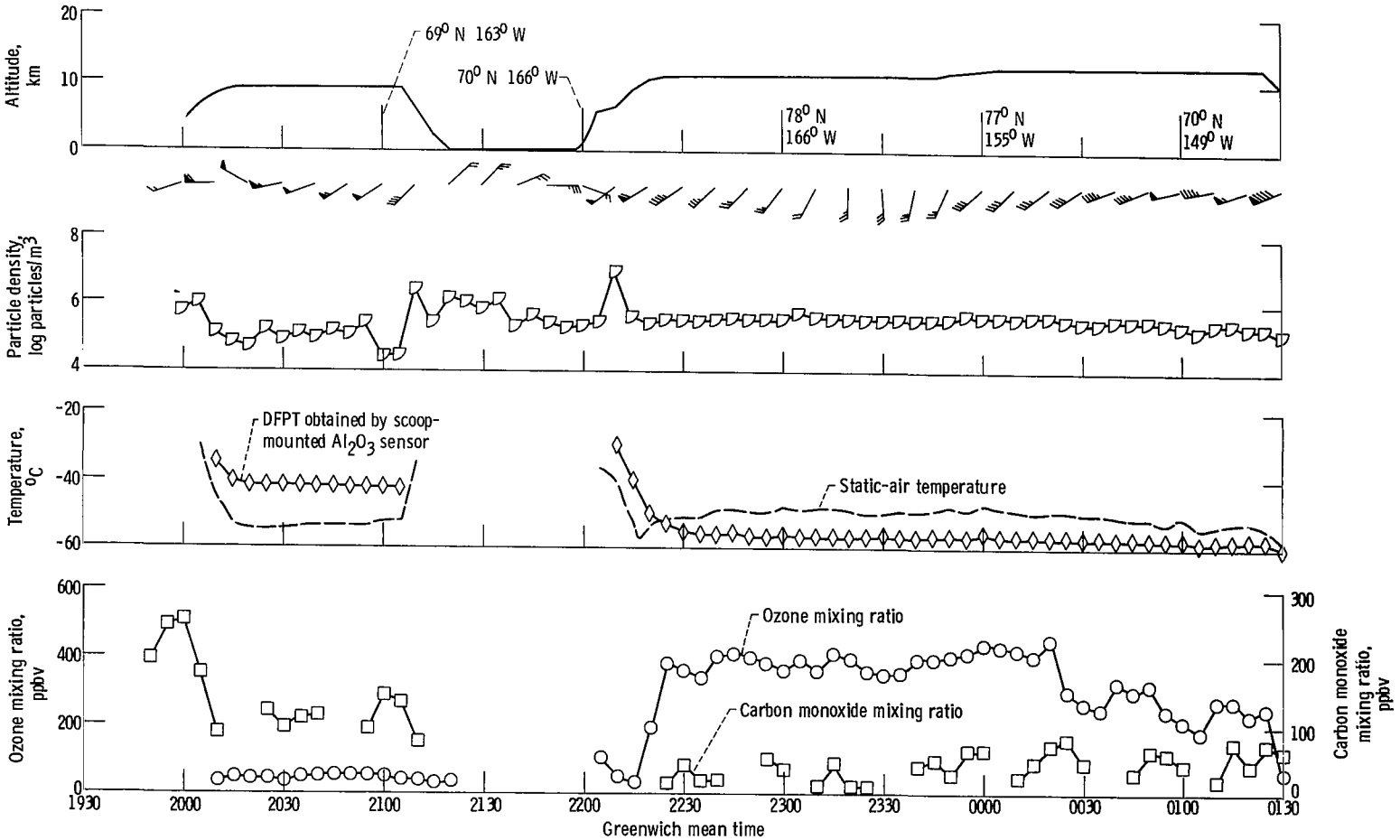

(d) Flight 9: October 22, 1975, Fairbanks to Fairbanks.

Figure 17. - Continued.

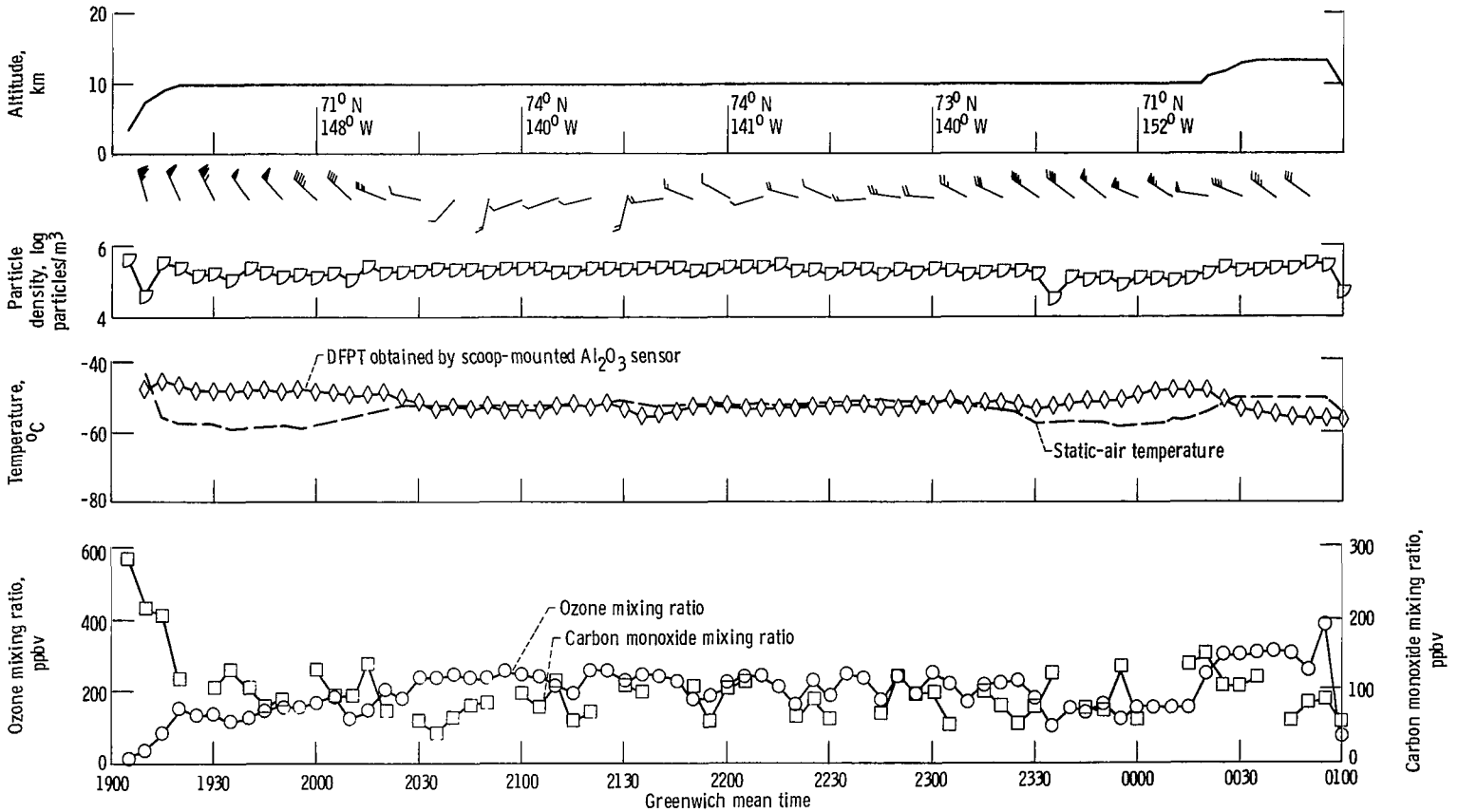

(e) Flight 12: October 26, 1975, Fairbanks to Fairbanks.

Figure 17. - Concluded.

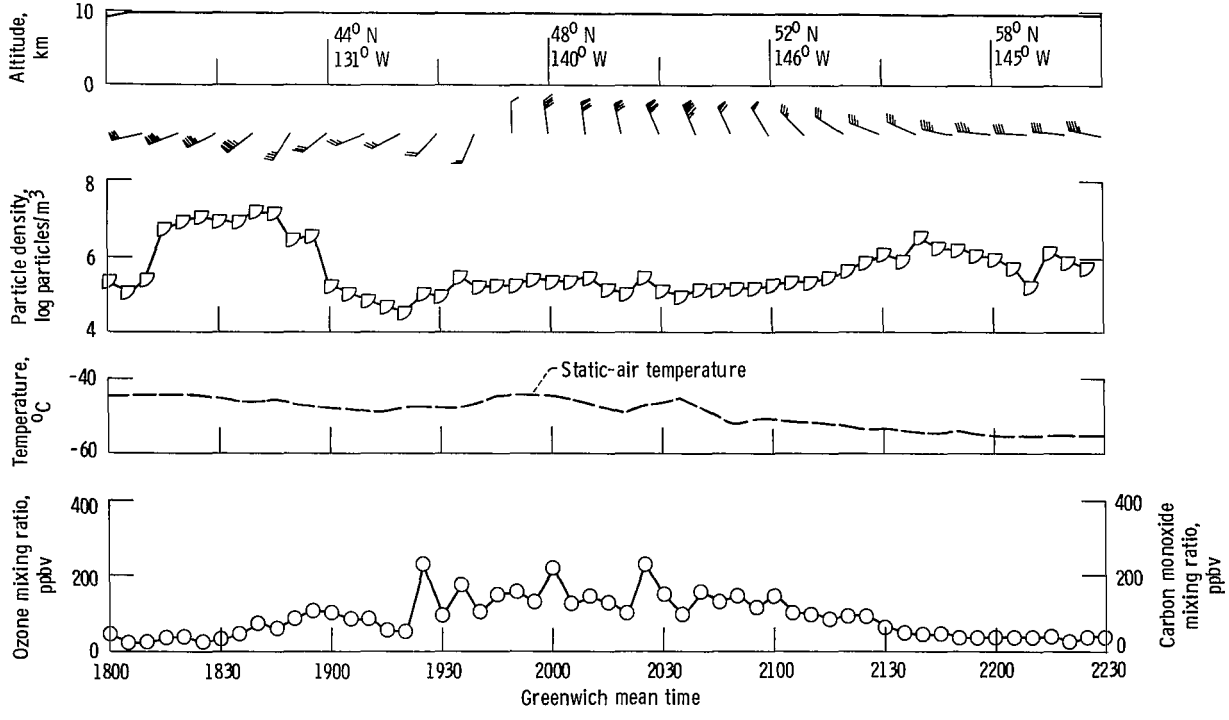

(a) Flight 2: October 8, 1975, Moffett Field to Fairbanks.

Figure 18. - Ferry flights for phase III.

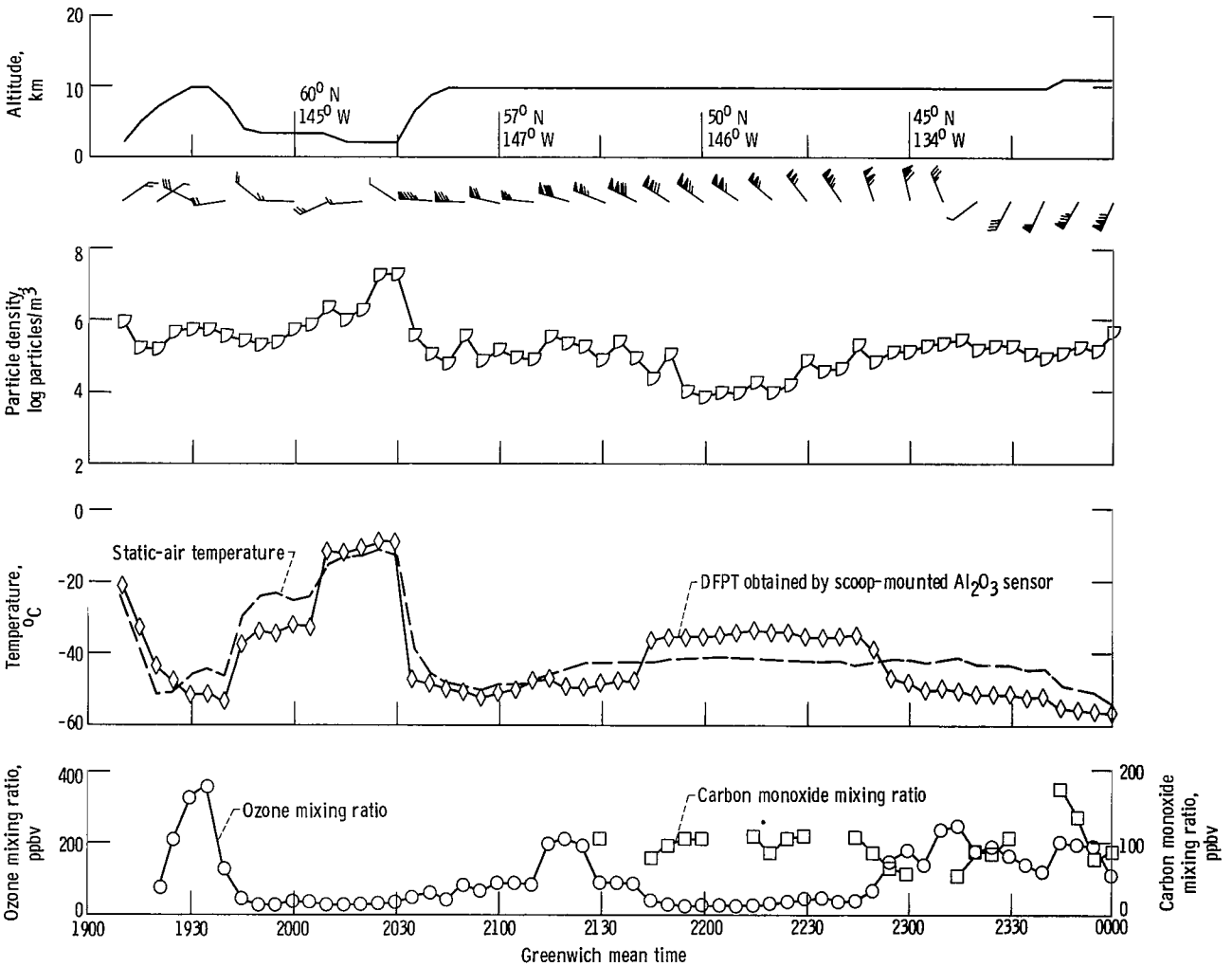

(b) Flight 14: October 29, 1975, Fairbanks to Moffett Field.

Figure 18. - Concluded.

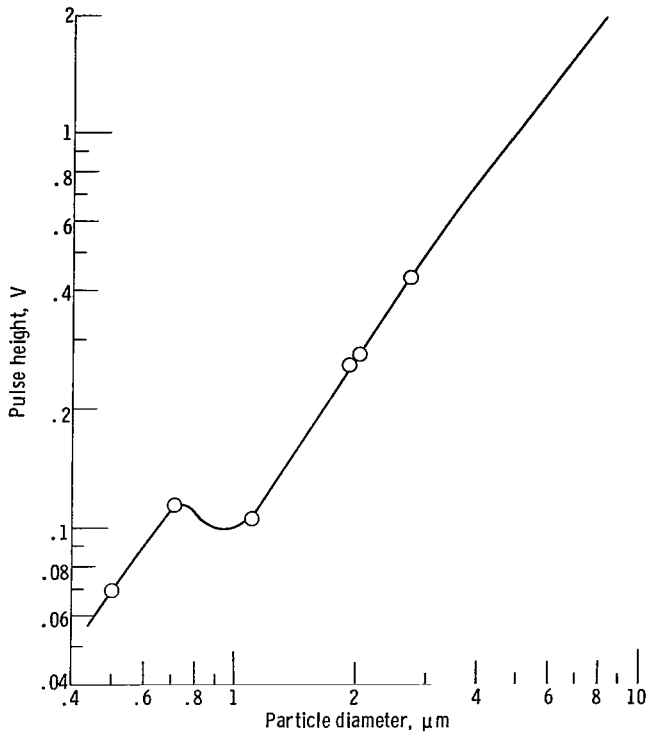

Figure 19. - Particle counter calibration.

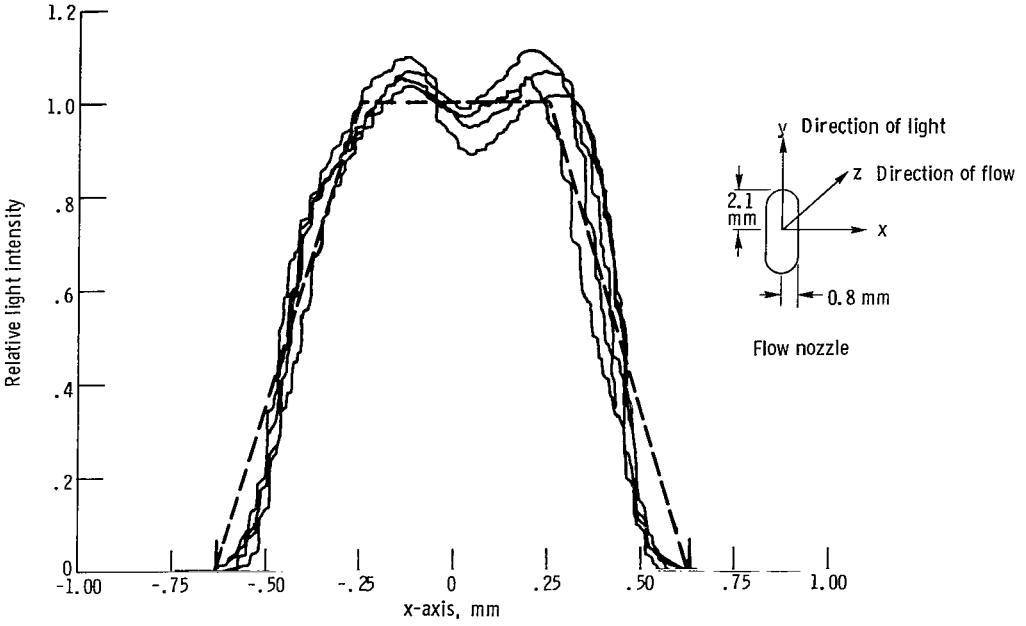

Figure 20. - Relative light intensity as function of distance along x-axis. The four curves cover a 2-millimeter-distance along y-axis. Count correction based on dashed curve.

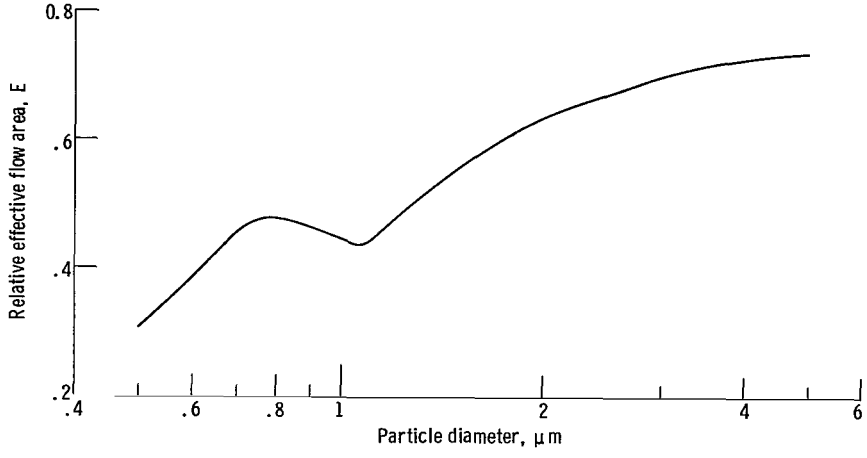

Figure 21. - Relative effective flow area as function of particle diameter based on a 0.07-volt discriminator level, the dashed curve in figure 1, and the calibration curve in figure 2.

"The aeronautical and space activities of the United States shall be conducted so as to contribute . . . to the expansion of human knowledge of phenomena in the atmosphere and space. The Administration shall provide for the widest practicable and appropriate dissemination of information concerning its activities and the results thereof."

—NATIONAL AERONAUTICS AND SPACE ACT OF 1958

NASA SCIENTIFIC AND TECHNICAL PUBLICATIONS

TECHNICAL REPORTS: Scientific and technical information considered important, complete, and a lasting contribution to existing knowledge.

TECHNICAL NOTES: Information less broad in scope but nevertheless of importance as a contribution to existing knowledge.

TECHNICAL MEMORANDUMS: Information receiving limited distribution because of preliminary data, security classification, or other reasons. Also includes conference proceedings with either limited or unlimited distribution.

CONTRACTOR REPORTS: Scientific and technical information generated under a NASA contract or grant and considered an important contribution to existing knowledge.

TECHNICAL TRANSLATIONS: Information published in a foreign language considered to merit NASA distribution in English.

SPECIAL PUBLICATIONS: Information derived from or of value to NASA activities. Publications include final reports of major projects, monographs, data compilations, handbooks, sourcebooks, and special bibliographies.

TECHNOLOGY UTILIZATION PUBLICATIONS: Information on technology used by NASA that may be of particular interest in commercial and other non-aerospace applications. Publications include Tech Briefs, Technology Utilization Reports and Technology Surveys.

Details on the availability of these publications may be obtained from:

SCIENTIFIC AND TECHNICAL INFORMATION OFFICE

NATIONAL AERONAUTICS AND SPACE ADMINISTRATION

Washington, D.C. 20546